EUFIND:

EUROPEAN ULTRAHIGH-FIELD IMAGING NETWORK FOR NEURODEGENERATIVE DISEASES

Report of a JPND Working Group on Harmonisation and Alignment in Brain Imaging Methods

April 2018

JPND research

EU Joint Programme – Neurodegenerative Disease Research

Joint Programming Neurodegenerative Disease:

Harmonisation and Alignment in Brain Imaging Methods for Neurodegeneration

Working Group
European Ultrahigh-Field Imaging Network for Neurodegenerative Diseases (EUFIND)

Final Report

Content

1. Executive Summary

Magnetic resonance imaging (MRI) measures of brain structure and function form important pillars in the assessment of dementias. There is a strong need to advance MR imaging to produce more sensitive and more specific biomarkers of neurodegeneration and to test new approaches to study pathology and its functional consequences. At the prevalent field strength of 3 Tesla, progress in these areas has plateaued. Therefore, there is considerable interest to explore and develop the potential utility of ultrahigh-field MRI at 7 Tesla for neurodegeneration research. With the emerging availability of 7T technology across Europe it is timely to resolve which clinical and scientific opportunities should be prioritised for collaborative research and how these imaging developments can be harmonised in a world-leading European 7T imaging network. In our working group, the European Ultrahigh-Field Imaging Network in Neurodegenerative Diseases (EUFIND), representatives of 22 sites (comprising all vendors) across Europe with leading MRI and dementia experts have agreed to join forces to identify opportunities and challenges of 7T MRI and to draw a roadmap for implementing and reporting harmonised ultrahigh-field MRI in dementia.

The major focus of EUFIND is Alzheimer's Disease (AD) but with experts in Parkinson's Disease (PD) in the working group we have the opportunity to optimise and harmonise across these two most common neurodegenerative disorders (as well as discussing extensions to other neurodegenerative diseases). We also interact with the JPND working group for harmonising MRI in vascular dementia by having shared contributors (HARNESS).

Members of the EUFIND group have a demonstrated track record in cutting-edge 7T- and dementia-imaging research. Our discoveries indicate that 7T MRI has the potential to advance research in neurodegeneration at several levels. 7T MRI allows very high structural resolution, quantitative anatomy, and providing more sensitive and accurate detection of volume changes (Maass, 2015; Hoffmann, 2012; Lusebrink, 2013) and atrophy than 3T MRI, especially relevant to the detection of pre-symptomatic change and short-term experimental medicines studies. It also allows submillimetre resolution in functional imaging enabling layer-specific functional imaging (Speck, 2008; Maass, 2014) and functional connectivity assessment of small cortical regions such as entorhinal subdivisions (Maass, 2015). The higher field strength is a major benefit for imaging macromolecular changes such as iron deposition (Wharton, 2010; Deistung, 2013), for fine-grained diffusion imaging tractography (Vu, 2015; Foxley, 2014), for spectroscopy (Lunghi, 2015; Tkac, 2009; Emir, 2016) and for multinuclear spectroscopy of inflammatory and metabolic processes (based on sodium, potassium, chlorine spectra) (Zaiss, 2016; Biller, 2016). Other important applications of 7T are imaging intra-cortical and vascular pathology (Jouvent, 2011; De Guio, 2014; De Guio, 2014; Drouin-Ouellet, 2015; Bouvy, 2015; Wisse, 2015; van Veluw, 2013}, high resolution angiography (Radbruch, 2014), vessel wall imaging (Viessmann, 2016) and delineation of subcortical and brain stem structures as well as differentiation of cellular layers (Boutet, 2014). EUFIND also comprises major experts in the field of MR sequence development and image analysis affording us with the opportunity to explore novel 7T imaging techniques (including quantitative imaging, perfusion measures, high-resolution venography). There is considerable expertise in the group for establishing large scale MRI networks with harmonised protocols, SOPs and quality assurance (e.g., German Ultrahigh-Field Imaging GUFI (Ladd, Speck), the UK Medical Research Council's UK7T Network (Rowe, Bowtell, Jezzard, Wise, Goense), the German National Neuroimaging Network in the DZNE (Duzel, Speck, Nestor, Stöcker), the CATI National Neuroimaging Network in France (Mangin, Chupin). A first GUFI-study has demonstrated the multi-centre feasibility of 7T.

The EUFIND working group thus brings together comprehensive leading expertise for identifying in which of these clinical and scientific areas 7T offers improvements over 3T and where it has the potential to become an indispensable tool. EUFIND constitutes the largest 7T network worldwide. Consensus in this group led to the development of a tractable and high-impact roadmap for neurodegeneration research.

2. Objectives and Approach of the Working Group

The specific objectives of EUFIND concern clinical application and research using 7T MRI. For clinical applications which in EUFIND focus on Alzheimer's disease and Parkinson's Disease, the objectives are

- To enable rapid implementation of large multi-site and multi-vendor studies in order to be able to address clinically relevant questions
- To utilize the multi-disciplinary nature of EUFIND towards clinical studies that integrate information about structure, function, vascular and molecular pathology
- To establish a multidisciplinary network that facilitates the identification of clinical „key applications" and „use cases" for 7T
- To set up a trial-ready network with sensitive imaging outcome biomarkers and sensitive lesion detection
- To enable comparative studies between different diseases (also beyond AD and PD)
- To accelerate change detection and to decrease sample sizes in trials by achieving best possible sensitivity and signal to noise

For research, the objectives are

- To disseminate knowledge between centers and enable joint research projects
- To develop methods for integrating data about structure, function, vascularization, molecular, metabolic and macromolecular status of tissue
- To narrow the gap between animal and human studies through higher resolution
- To enable and validate multi-center, multi-vendor research studies at 7T

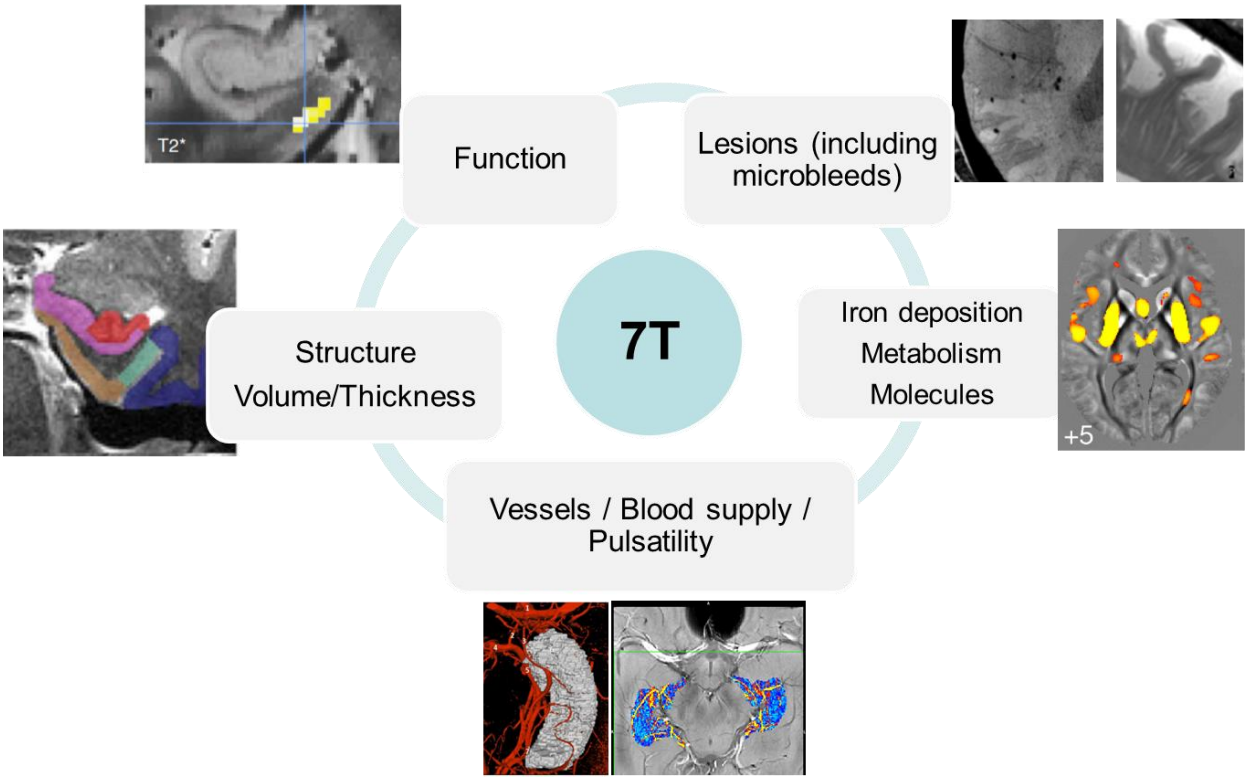

The integrative and multidisciplinary nature of EUFIND

The EUFIND Working Group has conducted two meetings, several telephone conferences and continues its efforts beyond the end of the JPND funding with a third meeting in January 2018. The timeline of the Working Group meetings and the miles-stones for objectives were as follows:

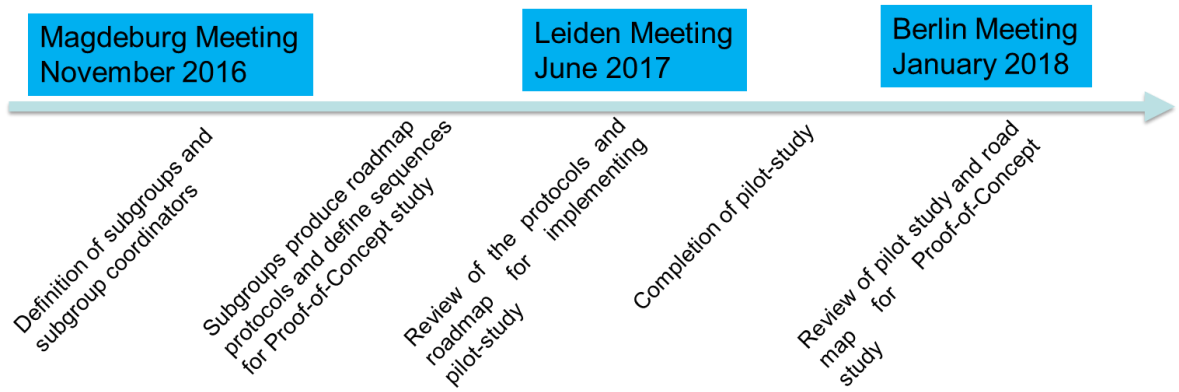

During the first EUFIND Meeting in Magdeburg (November 2016), the Working Group defined 7 subtopics (see below) and elected subtopic coordinators. A Steering Committee was appointed comprising the EUFIND coordinators, the subgroup coordinators and representatives of each country.

For each subgroup, a list of interested scientist members was identified who then focussed on the specific issues and questions related to the subgroups. After the Magdeburg Meeting, subgroups defined topics of interest, discussed a roadmap how these topics could be addressed and developed recommendations for a scanning protocol for a pilot-study across 7T sites.

Steering Committee

Emrah Düzel, Oliver Speck, Julio Acosta-Cabronero, Geert Jan Biessels, Isabella Björkman-Burtscher, Michel Bottlaender, Richard Bowtell, Mark v Buchem, Dennis Chan, Stuart Clare, Ariane Fillmer, Penny Gowland, Oscar Hansson, Jeroen Hendrikse, Oliver Kraff, Itamar Ronen, Esben Petersen, James Rowe, Hartwig Siebner, Tony Stoeker, Michela Tosetti, Kamil Uludag, Alexandre Vignaud, Jaco Zwanenburg

In the EUFIND Meeting in Leiden (June 2017, see photo below), the subgroup coordinators presented their progress and on the basis of each subgroup' recommendations a sequence protocol for a pilot-study was developed. During this meeting all sites agreed to perform a multi-centre pilot study and thus exceed the original JPND project plan by applying the pilot protocol in a number of subjects, combine all data and perform a first analysis. All groups agreed to participate and contribute "in kind".

This protocol combines high resolution structural imaging sequences for morphometric information (structural T1 and T2 sequences), a sequence to image vascular pulsatility (2D phase), a high resolution functional resting state fMRI sequence, a quantitative susceptibility weighted sequence to image iron pathology and venous oxygen saturation, and a proton-spectroscopy sequence. The details of the protocol are as follows (see subgroup reports for details and vendor-specific variations of this protocol):

Sequence description	**Resolution (mm)**	**Acquisition time**
Structural T1	0.65 isotropic	8:14
MR 2D phase	.3 x .3 x 2	~ 5:00
Resting state fMRI – Inverted Phase	1.1 isotropic	0:24
Resting state fMRI	1.1 isotropic	10:27
QSM	.35 x .35 x 1.25	8:46
High resolution T2 hippocampal angulated	.4 x .4 x1 mm	7:47
MR spectroscopy	20 x 20 x 20	Tbd

In the following sections, we introduce the subtopics and their work in more detail.
Each subgroup provided preliminary results obtained in this pilot study together with topic specific recommendations for a roadmap.

3. Recommendations and Roadmaps

A. Clinical applications

***Subgroup coordinators**: Marc v Buchem, Emrah Düzel, Oscar Hansson, Hartwig Siebner*

The clinical subgroup is focused on overarching goals pertaining to the potential of 7T in clinical applications by integrating across all other subgroups. Where possible we identified short-term clinical goals that are achievable with existing technology and long-term clinical goals which include foreseeable applications that require additional technological development over the next years. In doing so, we made a distinction between "*clinical routine*" and "*clinical research*".

Clinical routine

The utilization of 7T in clinical routine is in its infancy due to regulatory constraints. This may change in the near future given the approval of a first 7T system by the US Food and Drug Administration (FDA) for clinical use:

https://www.fda.gov/NewsEvents/Newsroom/PressAnnouncements/ucm580154.htm.

We structure the considerations for potential applications of 7T in clinical routine into those that may benefit from the high-resolution which can be achieved with 7T and those that are related to the possibility of increasing the speed of acquisition rather than resolution. Finally, we distinguish between diagnostic and prognostic imaging.

High resolution:
As outlined in the Highest Resolution Morphometry section, very high resolution structural imaging has the potential to provide detailed spatial information about neurodegeneration. This makes 7T potentially relevant for imaging small predilection structures for neurodegenerative pathology, such as the locus coeruleus, midbrain nuclei, subregions of the entorhinal cortex and the subfields of the hippocampus. Currently, the widespread use of such imaging at 7T in patients with neurodegenerative disease is not feasible in clinical routine because movement artifacts that are common in this population cannot be readily controlled and eliminated. Only a few 7T centers have sophisticated movement correction methods (i.e. prospective movement correction) implemented and the utility of these methods in routine assessment is limited due to technical challenges.

Ultra-fast acquisition:
As outlined in the Highest Resolution Morphometry section, the increased signal to noise ratio provided by 7T is not only beneficial for increasing resolution. The gain can also be used for speeding acquisition at resolutions that are typically used at 3T. This might be of interest in neurodegeneration where ultra-fast acquisition would strongly contribute to a reduction in movement artifacts. It could also contribute to achieving higher through-put in routine imaging and to improving image quality in pharmacological trials with patients who are prone to movement. Such sequences are being developed and could be available for wider use within a few years.

Diagnostic imaging:
There is no diagnostic MRI sequences for neurodegenerative diseases. It is not foreseeable that MRI sequences at 7T can replace molecular imaging biomarkers or CSF. Some techniques such as QSM may become relevant in the future but this requires substantial research and development. Diagnostic use cases are nevertheless possible and EUFIND is an ideal setting to identify such use-cases because most 7Ts in EUFIND are linked to a clinical setting and a direct comparison to a routine 3T assessment is feasible. Use-cases that were discussed among EUFIND members as being within reach of current 7T technology include

- *Epilepsy*: to determine whether in cases that are MRI negative at 3T, 7T can help identifying a lesion
- *Microbleeds*: to determine whether microbleeds not visible with 3T can be identified with 7T
- *Differential diagnosis*: to determine whether there is a potential to separate PSP, MSA and CBD and PD, or AD and LBD from each other. This could be aided by imaging small structures such as the subtantia nigra or locus coeruleus. However, we also note that diffusion tensor imaging which can potentially distinguish widespread taupathies from other neurodegenerative conditions may not strongly benefit from 7T.
- *Deep Brain Stimulation (DBS)*: 7T could improve the accuracy of identifying the motor area of the subthalamic nucleus and thereby help improving target placement for DBS.

Prognostic imaging:
Using Amyloid-PET or CSF data the molecular Alzheimer's disease signature can be identified up to 20 years before the onset of dementia (assessment of disease state). For a patient who presents with subjective cognitive complaints (SCD) or a mild cognitive impairment (MCI) for clinical assessment and shows evidence of amyloid pathology the major challenge is to determine when dementia symptoms are likely to emerge (i.e. in 1, 5 or 10 years). Here high-resolution MRI could potentially help to provide such prognostic information by revealing the stage of neurodegeneration. In addition, repeated high-resolution MRI to obtain a trajectory for the rate of neurodegeneration in less than a year (similar to staging in cancer treatment) could be feasible with 7T but expensive with Tau-PET and Amyloid-PET.

Clinical research

There are a number of opportunities for utilizing 7T in clinical research. For instance, very high resolution structural imaging could be more informative in discovering and characterizing neurodegeneration and thereby determining to what extent tau and amyloid pathology measures with PET or CSF are associated with neurodegeneration. We have identified the following topics for clinical research:

- *Functional consequences of brain pathology:* High resolution fMRI can inform about top-down and bottom-up consequences of brain pathology on brain function and this would be particularly the case if resolution would be high enough (around 1 mm) to resolve activity in different cortical layers to determine the directionality of functional interactions. In addition, task fMRI could be used to probe the cognitive function of

specific brain regions, such as subregions of the entorhinal cortex, subfields of the hippocampus, the locus coeruleus and basal ganglia circuits. Such information could be useful to understand the impact of pathology on defined cognitive functions but also to probe target engagement in drug trials.

- *Relationship to molecular biomarkers*: Whether or not 7T MRI can provide indirect information about amyloid plaque deposition is still unclear and any such methods would require years for validation. However, Aß pathology which occurs 10-20 years before symptom onset initially causes very little structural damage before tau pathology develops. Tau pathology, in turn, is assumed to be associated with neurodegeneration. For a better understanding of how neurodegeneration progresses along-side the interaction of amyloid and tau-pathology, higher resolution could be beneficial. For that purpose, MRI could potentially replace tau-PET where it is not available.
- *Determining the trajectory of neurodegeneration:* Longitudinal multi-parametric high-resolution MRI could be used to develop a mathematical model of disease progression (similar to staging in cancer treatment). Such model information could be very informative in drug trials and would be very expensive to achieve with Tau-PET.
- *Non-amyloid/non-tau pathology:* 7T MRI can also improve the detection of other types of pathologies in the brain and thereby complement information from PET on tau and parenchymal amyloid-plaque aggregates. One example is vascular pathology. That way 7T's high resolution may help improving the detection of comorbidities.
- *Differential diagnosis:* We see a potential for 7T imaging to help improving the differential diagnosis of different neurodegenerative diseases (i.e PSP, MSA and CBD and PD).
- *Outcome markers in proof-of-concept clinical trials:* Increased sensitivity to quantify neurodegeneration could be beneficial for a neurodegeneration read out in drug trials.

Roadmap
(required method development and implementation)

We agreed that a roadmap for implementing 7T in a clinical setting needs to accompany the ongoing and productive methods development in the 7T field. We foresee a four-step process:

First, common sequences and SOPs need to be implemented as per the recommendations from the other subgroups. This process is almost completed in EUFIND.

Second, a proof-of-concept study needs to be conducted with healthy older adults in the age-range spanning the preclinical phase of AD (>50 - 70 years).

Third, a first clinical study with MCI, early AD or PD patients needs to be conducted to establish the planned readouts in a clinical population.

Fourth, on the basis of the developments achieved in phases 1 to 3, use-cases can be developed by

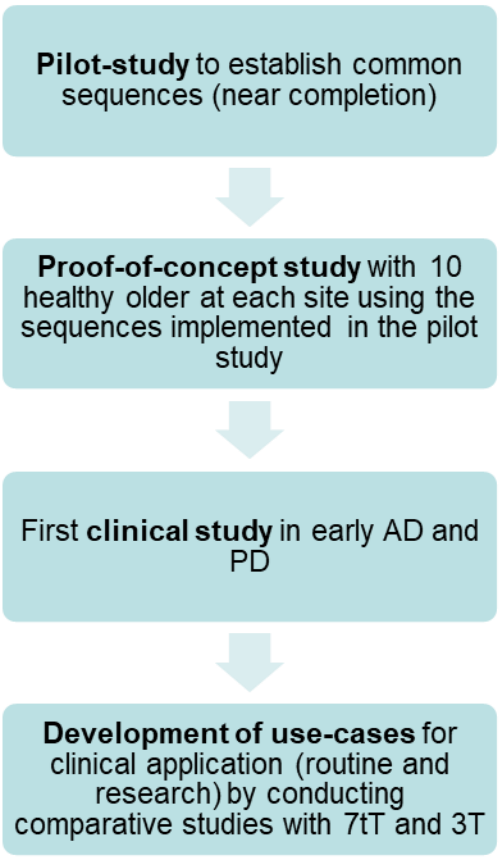

conducting comparative studies in EUFIND using 3T and 7T.

Subgroup contributors

Nin Bajaj, Michel Bottlaender, Isabella Björkman-Burtscher, Hugues Chabriat, Dennis Chan, Olivier Colliot, Mirco Cosottini, Bruno Dubois, Daniela Frosini, Graziella Donatelli, Francois De Guio, Cornelius Deutschl, Martin Dichgans, Gwenaelle Douaud, Emrah Duzel, Stéphane Epelbaum, Oskar Hansson, Heidi Johansen-Berg, Eric Jouvent, Kim Graham, Oliver Kraff, Mark Ladd, David Linden, Annemette Løkkegaard, Clare Mackay, Armin Nagel, Peter Nestor, Thoralf Niendorf, Oliver Peters, Harald Quick, James Rowe, Marie Sarazin, Matthias Schroeter, Hartwig Siebner, Maria Stefanescu, Tony Stöcker, Yasin Temel, Philip Thomann, Betty Tjims, Alexandre Vignaud, Arno Villringer, Adam Waldman, Joanna Wardlaw, Andrew Webb, Nikolaus Weiskopf

B. Highest resolution anatomy

***Subgroup coordinators**: Dennis Chan, Tony Stöcker*

The goals of this subgroup were divided into short term **"**What we can do in JPND with current systems and methods?" and long term "What requires significant future effort?" issues to be addressed within separate Work Packages (WPs).

WP1 focused on regions of interest (ROI) segmentation and was subdivided into three components. WP1a focused on pre-selection of ROIs on the basis of their early involvement in neurodegenerative diseases (locus coeruleus and medial temporal lobe subregions in Alzheimer's disease, substantia nigra and basal ganglia in Parkinson's disease, amygdala in frontotemporal dementia). All are small anatomically, and as such it is proposed that the higher resolution of 7T permits segmentation with a degree of accuracy required for disease detection that is unachievable at lower field strengths. The current ROI list is not fixed, but represents instead those regions for which segmentations at 7T have already been undertaken in previous work, which facilitates their initial study in EUFIND. ROIs for consideration in next stage work include the olfactory bulb, nucleus reuniens and the dorsal nucleus of the vagus nerve.

The objective of WP1b was to establish ROI segmentation protocols at 7T that would be associated with the smallest possible implementation effort across JPND. This involved initial identification of already available processing pipelines and segmentation approaches for highest resolution anatomy from T1 and T2 weighted images, including those for the medial temporal lobe (Berron et al 2017: Neuroimage Clinical 15, 466-482), substantia (Visser et al 2016: Neuroimage 139, 324-336) and basal ganglia (Lenglet et al. 2012: PLoS One 7(1):e29153). Where more than one protocol existed for any given ROI, a single protocol was selected for multi-site implementation within WP1c.

The objective of WP1c is to achieve multi-site implementation with protocols selected in WP1b for segmentation of target regions identified in WP1a. Three phases were identified:

1. Pilot phase
   - Implementation of selected ROI protocols at all sites
   - Acquisition of 1-3 test datasets per site
   - Data analysis with respect to quality, homogeneity, comparability across sites

2. Acquisition of normative datasets
   - Young adulthood (20-40)
   - Midlife (40-60)
   - Older age (60-80)

3. Small-n preliminary acquisition of disease datasets
   - Preclinical (eg presymptomatic Huntingdon's disease, preclinical Alzheimer's disease cohorts)
   - Clinical (symptomatic patients with established disease)

Methods

Image Acquisition: As stated above, the WP1 aims in establishing multicentre 7T high resolution anatomy imaging protocols. For this purpose, protocols of a T1-weighted whole brain acquisition as well as a T2-weighted ROI acquisition of the hippocampus were developed and implemented across all sites. Well-established methods were chosen which were available at all sites. Whole brain T1-weighted imaging was achieved at 0.65 mm isotropic resolution utilizing the 3D MP-

RRAGE sequence. The high resolution T2-scan was implemented as a 2D Turbo-Spin Echo (TSE) sequence at 0.4x0.4x1.0 mm resolution, where slices were oriented orthogonal to the long axis of the Hippocampus. The following table summarizes the details of the sequence implementation at the Siemens scanners within the EUFIND network. Minor system-specific deviations were present at the Phillips and GE scanners. T1 and T2 imaging data were acquired from 22 healthy volunteers, scanned across 13 sites.

T1-weigthed Whole Brain Imaging Protocol: 3D-MPRAGE Sequence

Resolution	0.65x0.65x0.65 mm	TI	1100 ms	Bandwidth	250 Hz / Pixel
FOV	267 x 226 x 166 mm	TR	2500 ms	TE	3.06 ms
Matrix	384 x 348 x 256	Flipangle	7°	Echo Spacing	7.5 ms
GRAPPA	2	RF duration (Nonselective)		PE ordering	linear
Ref. lines	48	• Excitation (11 bino WE)	0.6 ms	**Scan Time**	**8:54 min**
		• Inversion (hyp.-secant)	10 ms		

T2-weigthed Hippocampus Imaging Protocol: 2D-TSE Sequence

Resolution	0.437x0.437x1.0 mm	TE	76 ms	Echo Trains / Slice	57
FOV	224 x 224 x 60.5 mm	TR	8020 ms	HyperEcho Readout	
Matrix	512 x 512	Bandwidth	155 Hz / Pixel	RF duration (Gaussian VERSE)	
Slices	55 (10% gap)	Echo Spacing	15.2 ms	• Excitation	4 ms
Orientation	orth. to hippo long axis	Turbo Factor	9	• Refocussing	6 ms
				Scan Time	**7:47 min**

Sequence parameters of the high-resolution anatomical imaging protocol.

Image Analysis: Whole brain image segmentation was performed on the T1 scans (MPRAGE). First, bias field correction (Vovk et al, 2007) modified for UHF-data was performed to remove image inhomogeneity induced by the transmit field. Afterwards the standard Freesurfer analysis pipeline "*recon-all*" was carried out (Reuter et al, 2012). For image analysis of the T2-weighted scans, the subregional segmentation of the medial temporal lobe has been undertaken on the high resolution T2 scans through the hippocampal formation using the Automated Segmentation of Hippocampal Subfields (ASHS) protocol of Berron et al. (2017).

Results

Fig. 1 depicts two sample images of the T1-weighted MP-RAGE sequence acquired at two EUFIND sites (Bonn and Pisa) with 7T scanners from different vendors (Siemens and GE, respectively). The Figure displays the importance of bias field correction pre-processing, which provides spatially homogenous images as input for the whole brain segmentation. An example of the segmentation result with the standard Freesurfer analysis pipeline is depicted in Figure 2. Sample images of the T2-analysis are displayed in Figure 3, to illustrate inter-scanner consistency of the Hippocampus subfield segmentation. These initial analyses have revealed two acquisition problems. The first relates to excessive head motion, as shown in Figure 2, which is related to the bright CSF signal and often observed in T2-weighted scans. The second problem is that of signal loss from the inferior temporal lobe. This is for instance illustrated in the Paris scan (Figure 3 right), which could potentially compromise segmentation of the most inferior subregions such as areas 35 and 36.

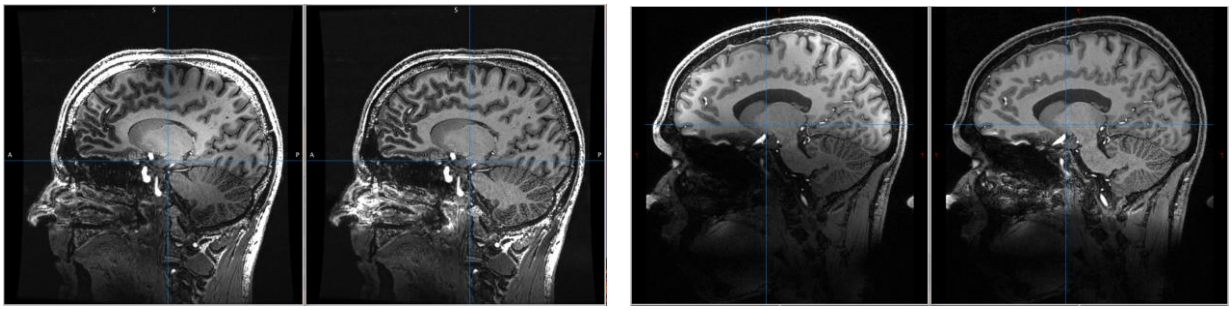

Figure 1. *Sample T1-weighted scans from two different sites (Left: Pisa, Right: Bonn). The respective images on the left display the original data as coming from the 7T scanners whereas the images on right shows the spatially homogenized results after bias field correction, as required for the Freesurfer analysis.*

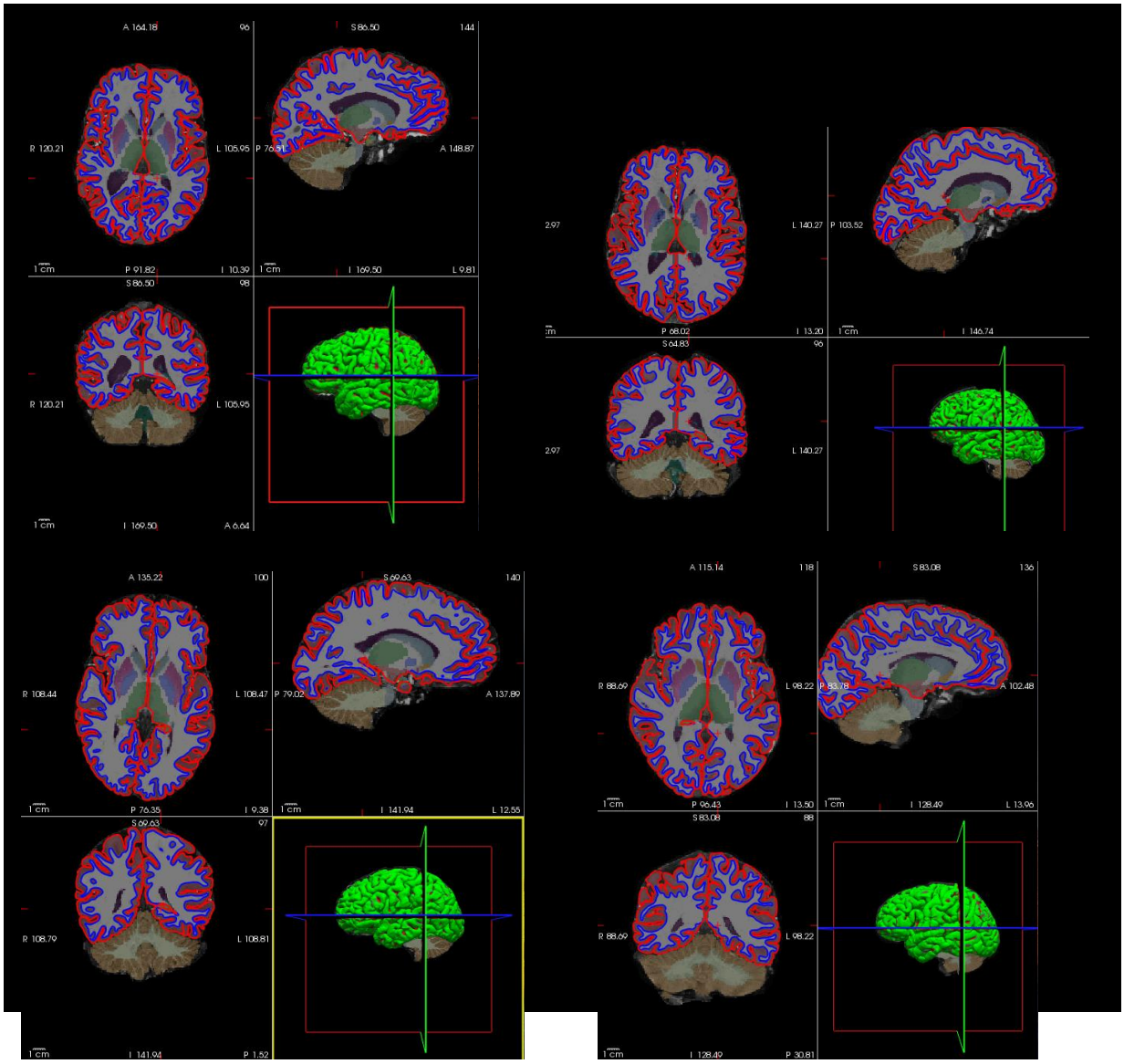

Figure 2. *Sample Freesurfer segmentation results of the high-resolution whole brain T1-scan from four sites (top left: Bonn, top right: Essen, bottom left: Magdeburg, bottom right: Paris). The figure shows that the multicenter 7T MPRAGE scans can be successfully processed with state-of-the-art analysis tools.*

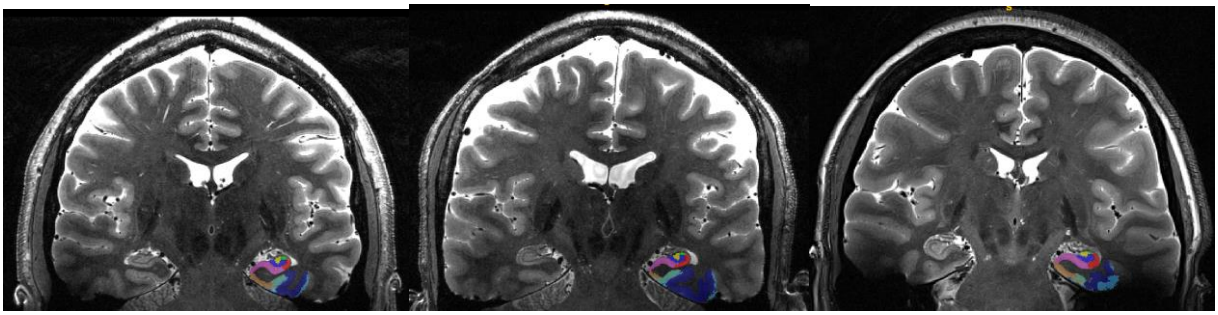

***Figure 3**. Coronal MRI scans through the body of the hippocampus, immediately distal to the hippocampal head. Scans acquired from Leipzig (left), Magdeburg (middle) and Paris (right). Colour legend of segmented regions: entorhinal cortex – brown, Brodmann area 35 – teal, Brodmann area 36 – dark blue, subiculum – mauve, CA1 – red, CA2 – green, CA3 – yellow, dentate gyrus – blue.*

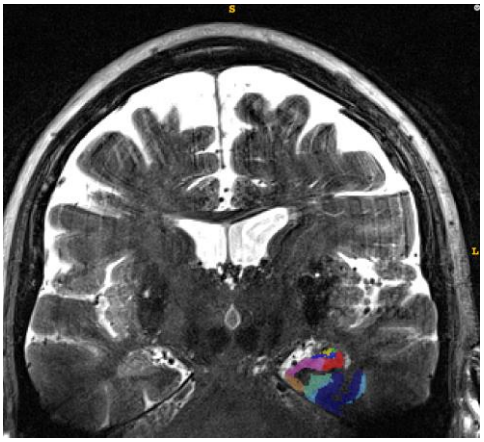

***Figure 4**. Visible motion artefact from a scan acquired at the Heidelberg site. Note, however, the ability of ASHS to yield subregional segmentation despite the presence of this artefact.*

Conclusions

Two high resolution imaging sequences to study brain anatomy were successfully implemented and tested in at least two subjects at 13 EUFIND sites. The analyses showed satisfactory segmentation results, both for the whole brain T1-scan as well for the Hippocampus T2-scan. However, reliable whole brain segmentation of 7T data requires appropriate pre-processing (bias field correction) in order to utilize the gold-standard brain segmentation tool Freesurfer.

The T2 pilot scan study demonstrated that overall satisfactory subregional segmentations of the Hippocampus were obtained when ASHS was applied to a number of different scans acquired from different sites. Motion and image inhomogeneity remain a problem for high resolution imaging at 7T. For the specific example of the T2-scan, both problems were observed in several scans of the pilot data. A possible quick remedy was proposed by means of a 3-fold accelerated acquisition with three repetitions using different transmit power. Subsequent averaging maintains SNR in comparison to the original protocol whereas motion artefacts are strongly reduced and, furthermore, transmit inhomogeneity is slightly reduced. This option has already been trialled at two scan sites and further comparison of the resultant scan quality with that acquired from a single acquisition will be required before implementation across all scan sites.

More general long-term solutions include use of prospective motion correction (McLaren et al, 2013) and utilization of parallel transmission in order to homogenize the transmit field at 7T,

where recent achievements show high potential for standardized application in a multicenter studies (Gras et al, 2017). Additionally, other promising acquisition and analysis methods for high resolution anatomical imaging will be explored in the future. Most importantly, it is of high interest to acquire complementary information such as structural connectivity from diffusion MRI and/or quantitative MRI such as relaxation time mapping or contrasts, which correlate with brain myelinisation. Moreover, in order to achieve these goals in clinical acceptable scan time, the high SNR at 7T can be utilized to implement strongly accelerated sequences. Here, novel sampling schemes and advanced image reconstruction methods as for example the waveCAIPI concept (Bilgic et al, 2015) can be used to drastically reduce the scan time of individual sequences. Preliminary results suggest that high-quality waveCAIPI MPRAGE images at 0.6 mm isotropic resolution can be achieved in less than 4 minutes. However, a harmonized implementation of these approaches across all EUFIND 7T sites will require major efforts in the future.

References

1. Bilgic B, Gagoski BA, Cauley SF, Fan AP, Polimeni JR, Grant PE, Wald LL, Setsompop K. Wave-CAIPI for highly accelerated 3D imag- ing. Magn Reson Med 2015;73:2152–2162. 11.
2. Gras, V., Boland, M., Vignaud, A., Ferrand, G., Mauconduit, F., Bihan, D. Le, … Boulant, N. (2017). Homogeneous non-selective and slice- selective parallel-transmit excitations at 7 Tesla with universal pulses : a validation study on two commercial RF coils. PLoS ONE, 1–16.
3. Maclaren, J., Herbst, M., Speck, O., & Zaitsev, M. (2013). Prospective motion correction in brain imaging: A review. Magnetic Resonance in Medicine, 69(3), 621–636.
4. Reuter M, Schmansky NJ, Rosas HD, Fischl B. Within-subject template estimation for unbiased longitudinal image analysis. Neuroimage 2012;61:1402–1418.
5. Vovk, U., Pernuš, F., & Likar, B. (2007). A review of methods for correction of intensity inhomogeneity in MRI. IEEE Transactions on Medical Imaging, 26(3), 405–421.

Subgroup contributors

Isabella Björkman-Burtscher, David Berron, Arturo Cardenas-Blanco, Dennis Chan, Marie Chupin, Olivier Colliot, Mauro Costagli, Gwenaelle Douaud, Emrah Duzel, Penny Gowland, Heidi Johansen-Berg, Jean-Francois Mangin, Mark Ladd, Armin Nagel, Esben Thade Petersen, Kerrin Pine, James Rowe, Hartwig Siebner, Oliver Speck, Maria Stefanescu, Philip Thomann, Tony Stöcker, Maxim Terekhov, Laura Schreiber Alexandre Vignaud, Kamil Uludag, Guy Williams, Nikolaus Weiskopf

C. Functional imaging

Subgroup coordinators: *Kamil Uludag, Emrah Düzel, Hartwig Siebner*

Whole-brain functional magnetic resonance imaging (fMRI) is a powerful tool to measure brain dynamics and is widely used in basic research and clinical neuroscience. Numerous studies have confirmed the existence of networks of brain regions that are characterized by temporally coherent, low-frequency fluctuations in the blood oxygenation level dependent (BOLD) signal through direct and/or indirect anatomical connections across the brain.

Importantly, the magnitude and spatial specificity of the fMRI signal depend on – besides the contrast mechanism (T_2* or T_2) – on the field strength employed for the measurements (Uludag, Muller-Bierl, & Ugurbil, 2009). Here, the main advantage of higher field strength is the increased longitudinal magnetization (i.e. more protons that align with B_0) leading to increased intrinsic signal-to-noise (SNR, ~ $B_0^{1.65}$) and contrast-to-noise (CNR) ratios (Duyn et al., 2007; Norris, 2003; Pohmann, Speck, & Scheffler, 2016; Vaughan et al., 2001). Increasing B_0 allows, therefore, acquisition of higher resolution data than what is achievable at lower field strengths within the same imaging time and comparable SNR and/or CNR (Pfeuffer et al., 2002; Uludag & Blinder, 2017; Yacoub, Harel, & Ugurbil, 2008). As such, 7T provides advantages for the spatial specificity of the fMRI signal through improved segregation of signals originating from distinct anatomical substrates (e.g. microvasculature vs. large surface vessels vs. white matter) and facilitating the imaging of human brain function down to the columnar and laminar levels (Polimeni, Fischl, Greve, & Wald, 2010; Yacoub et al., 2008).

However, despite tremendous improvements, acquisition of fMRI data still suffers from physiology- and hardware-related challenges (e.g. SAR issues and B_0 inhomogeneities) that, in addition, affect the generalization of fMRI studies across imaging platforms (Ugurbil, 2017). Thus, the EUFIND project aims to develop and evaluate the feasibility of a standardized protocol across several 7T sites for task- and resting-state fMRI, focusing on the application in neurodegenerative diseases. For the current proof-of-concept study and the preliminary results presented here, we examined the utility of the initial proposed (resting-state) fMRI protocol to image the connectivity in the anterior-lateral vs. posterior-medial medial temporal lobe networks. To that end, resting-state data were analyzed using parahippocampal (PHC) vs. perirhinal (PRH) cortex seed regions based on automated segmentation (ASHS) to investigate integrity of entorhinal and hippocampal sub-regional connectivity as shown earlier by Maass, Berron, Libby, Ranganath, and Duzel (2015).

Materials & methods

T_2*-weighted gradient echo planar images (EPIs) functional MRI data were acquired using a 7T MR system at five different imaging sites for a total of eight subjects (see ***Table 1*** for details on the sequence parameters and ***Fig. 1*** for an overview of the different datasets). Additionally, an inverted phase acquisition with same parameters was acquired for distortion correction. Distortion correction was applied (i.e. using FSL's *topup* and *applytopup*) after coregistering each volume to the first volume (i.e. using FSL's *mcflirt*).

Table 1 - Acquisition parameters for proposed standardized fMRI protocol.

Acquisition parameters rs-fMRI	
Spatial resolution	1.1 mm isotropic
Nr. of slices	40 (covering midbrain and medio-temporal cortex, including hippocampus and parahippocampal gyrus)
Nr. of volumes	250
TR	2400 ms
TE	22 ms
Partial Fourier	6/8
GRAPPA	4
References lines	64
Acquisition time	10:27 min.

Seed-to-voxel correlational analyses was performed on the distortion and motion corrected fMRI data using the conn-toolbox (Whitfield-Gabrieli & Nieto-Castanon, 2012). Functional connectivity patterns of PRC or PHC seeds with the rest of the cortex were analyzed. See also Maass et al. (2015) for a description of the ROI's segmentation procedure. For each functional connectivity analysis, seed regions' average time series were generated as regressors of interest. As covariates of no interest, WM and CSF time series and subjects' realignment parameters were included to account for physiological noise and movements, respectively. Functional data were band-pass filtered for frequencies of 0.01–0.1 Hz. Bivariate correlations were computed, resulting in correlation coefficients maps. To perform a course group analysis, correlation maps were registered to the MNI atlas and averaged across subjects.

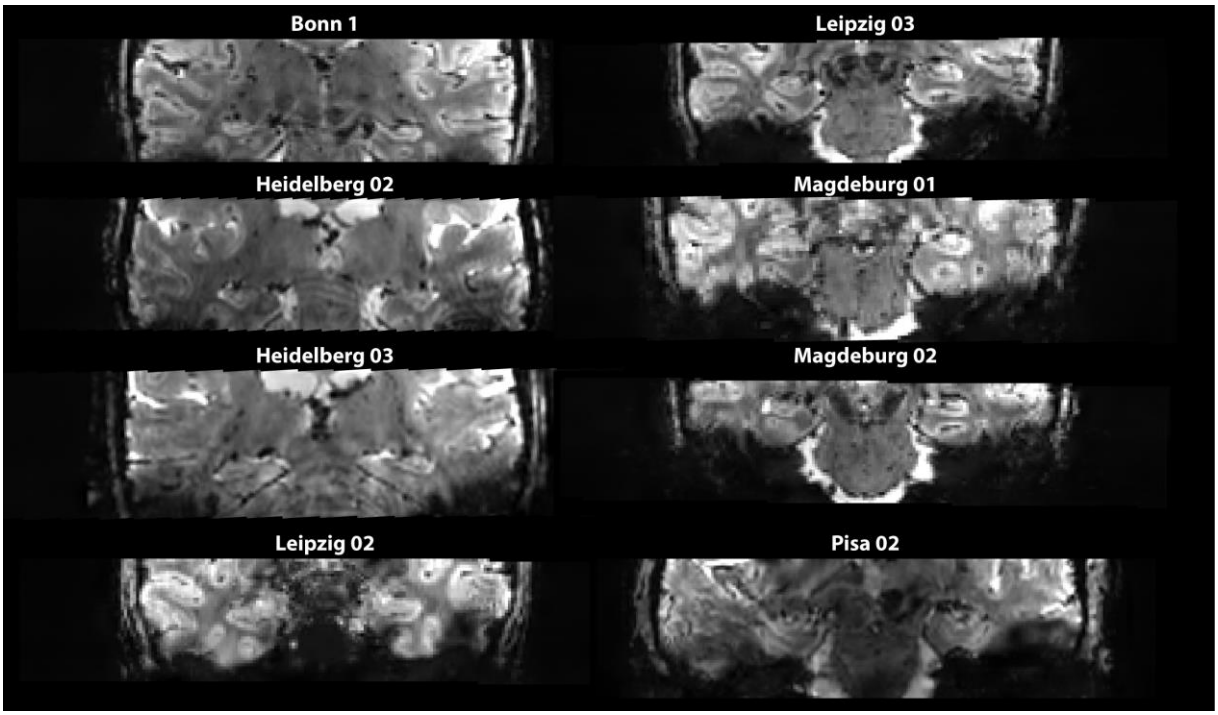

Figure 1. *Overview of subjects' mean EPI*

Results

A total of eight subjects, originating from five different imaging sites and vendors (i.e. Siemens and GE, only 'Pisa 02'), were analyzed. ***Fig. 1*** shows an overview of the subjects' mean EPI's in the coronal plane. Small differences can be observed across datasets with regards to the coverage of the imaging slabs, mainly due to slight variations in the slabs' orientation with respect to the anterior-to-posterior commissure axis in the sagittal plane. However, for all subjects the seeds ROI's could be reliably obtained and analyzed. Single-subject example 3D visualizations of the left hemisphere PHC (blue) and PRH (red) cortices are overlaid onto the T_2-weighted image in ***Fig. 2***. Evidently, both regions are located close to each other, however, the observed correlation maps exhibit different patterns (see the color-coded maps overlaid on the MNI template in ***Fig. 3***).

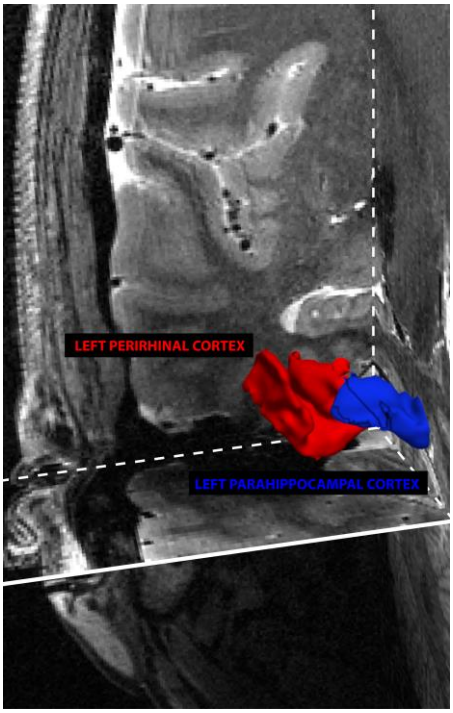

Figure 2. *3D visualization of the seed regions (perirhinal cortex, in red) and parahippocampal cortex, blue) overlaid onto a T_2 weighted image, for a single subject.*

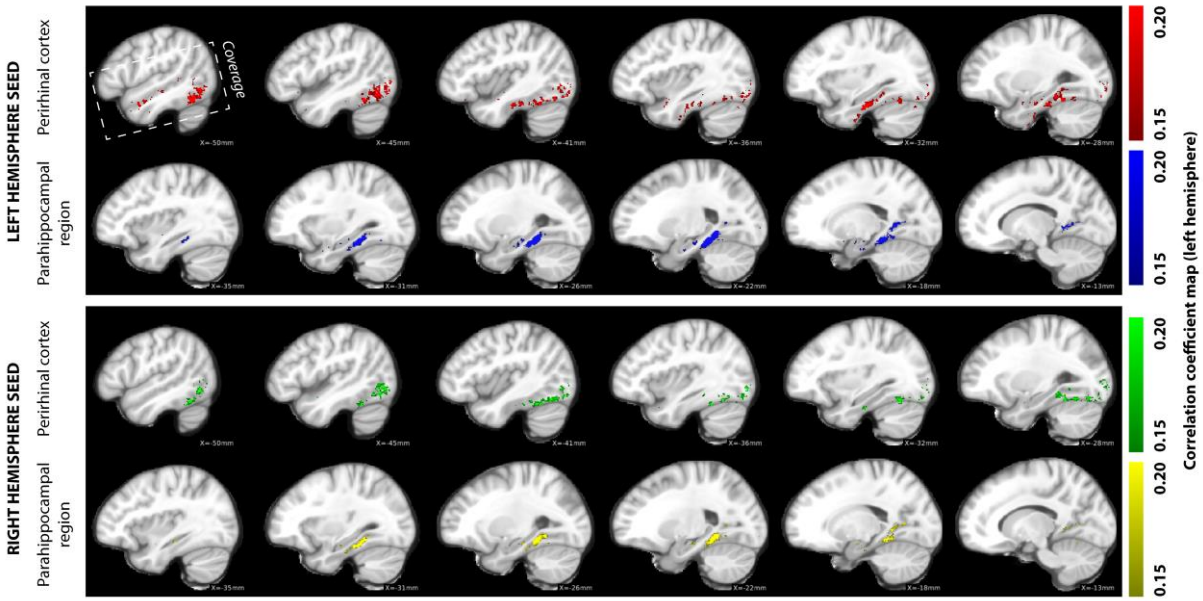

Figure 3*. Average functional correlation coefficient maps. Each seed region is color-coded (left hemisphere perirhinal cortex and parahippocampal region: red and blue, respectively and green and yellow for the right hemisphere, respectively).*

Conclusion

The current results show distinct functional brain connectivity for the PHC and PRH seeds as in earlier studies (Maass et al., 2015). However, the fMRI signal within the selected ROIs could have been affected differently across sites and subjects by the susceptibility artifacts that are observed near the inferior temporal lobes. This could have led to an increased inter-subject variation. In addition, analysis of more subjects, better inter-subject alignment and more detailed consensus on the slices' positioning will improve the current and/or future results (i.e. for the follow-up study).

References

1. Duyn, J. H., van Gelderen, P., Li, T. Q., de Zwart, J. A., Koretsky, A. P., & Fukunaga, M. (2007). *High-field MRI of brain cortical substructure based on signal phase.* Proc Natl Acad Sci U S A, 104(28), 11796-11801. doi:10.1073/pnas.0610821104.
2. Maass, A., Berron, D., Libby, L. A., Ranganath, C., & Duzel, E. (2015). *Functional subregions of the human entorhinal cortex.* Elife, 4. doi:10.7554/eLife.06426.
3. Norris, D. G. (2003). *High field human imaging*. J Magn Reson Imaging, 18(5), 519-529. doi:10.1002/jmri.10390.
4. Pfeuffer, J., van de Moortele, P. F., Yacoub, E., Shmuel, A., Adriany, G., Andersen, P., . . . Hu, X. (2002). *Zoomed functional imaging in the human brain at 7 Tesla with simultaneous high spatial and high temporal resolution.* Neuroimage, 17(1), 272-286.
5. Pohmann, R., Speck, O., & Scheffler, K. (2016). *Signal-to-noise ratio and MR tissue parameters in human brain imaging at 3, 7, and 9.4 tesla using current receive coil arrays.* Magn Reson Med, 75(2), 801-809. doi:10.1002/mrm.25677.
6. Polimeni, J. R., Fischl, B., Greve, D. N., & Wald, L. L. (2010). *Laminar analysis of 7T BOLD using an imposed spatial activation pattern in human V1.* Neuroimage, 52(4), 1334-1346. doi:10.1016/j.neuroimage.2010.05.005.
7. Ugurbil, K. (2017). *Imaging at ultrahigh magnetic fields: History, challenges, and solutions*. Neuroimage. doi:10.1016/j.neuroimage.2017.07.007.
8. Uludag, K., & Blinder, P. (2017). *Linking brain vascular physiology to hemodynamic response in ultra-high field MRI.* Neuroimage. doi:10.1016/j.neuroimage.2017.02.063.
9. Uludag, K., Muller-Bierl, B., & Ugurbil, K. (2009). *An integrative model for neuronal activity-induced signal changes for gradient and spin echo functional imaging*. Neuroimage, 48(1), 150-165. doi:10.1016/j.neuroimage.2009.05.051.
10. Vaughan, J. T., Garwood, M., Collins, C. M., Liu, W., DelaBarre, L., Adriany, G., . . . Ugurbil, K. (2001). *7T vs. 4T: RF power, homogeneity, and signal-to-noise comparison in head images*. Magn Reson Med, 46(1), 24-30.
11. Whitfield-Gabrieli, S., & Nieto-Castanon, A. (2012). Conn: *a functional connectivity toolbox for correlated and anticorrelated brain networks*. Brain Connect, 2(3), 125-141. doi:10.1089/brain.2012.0073.
12. Yacoub, E., Harel, N., & Ugurbil, K. (2008). *High-field fMRI unveils orientation columns in humans.* Proc Natl Acad Sci U S A, 105(30), 10607-10612. doi:10.1073/pnas.0804110105.

Subgroup contributors

Laura Biagi; David Berron; Dennis Chan; Mauro Costagli; Gwenalle Douaud; Emrah Duzel; Susan Francis; Roy Haast; Harald Moeller; Lars Nyberg; Oliver Speck; James Rowe; Hartwig Siebner; Tony Stöcker; Kamil Uludag; Nikolaus Weiskopf; Richard Wise; Greger Orädd

D. Vascular lesions / vascular system

***Subgroup coordinators**: Geert J Biessels, Jaco Zwanenburg, Esben Petersen*

7T MRI offers several unique opportunities to further our understanding of vascular contributions to neurodegenerative diseases. This includes both functional and structural assessment of the brain vasculature and parenchyma, as well as perfusion (Figure) [1][2]. EUFIND provides a unique environment to advance this area because several members of the Vascular lesions/vascular system subgroup are also members of the JPND HARNESS working group for harmonising MRI in vascular dementia.

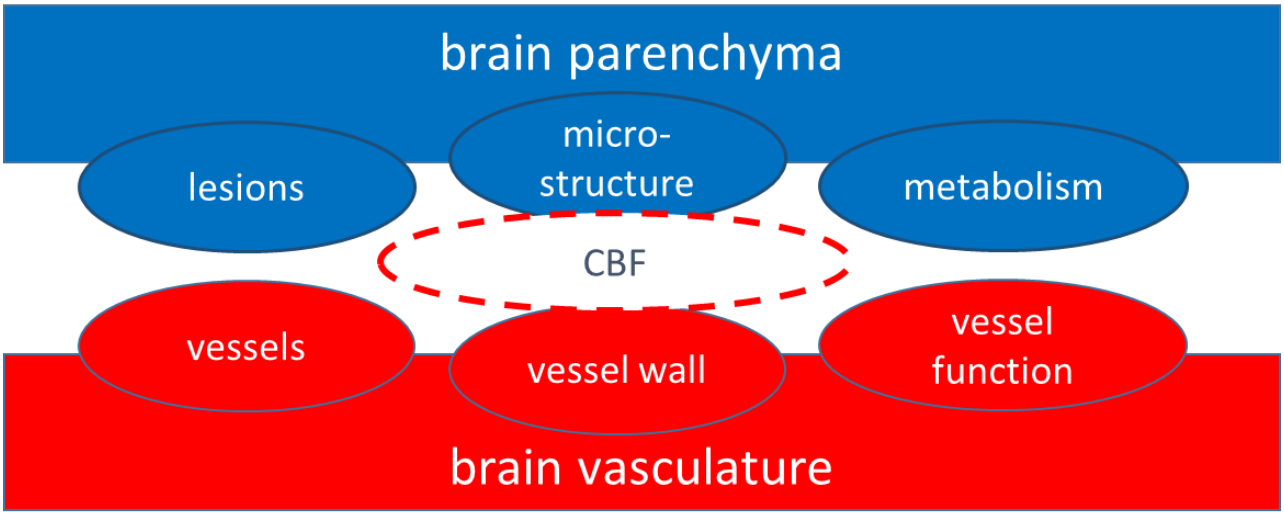

Vessels

- 7T MRI allows for high resolution imaging of both the arteries [3] (time-of-flight (TOF)) and the veins [4] [5] (T2* weighted imaging / susceptibility weighted imaging (SWI))
- Applicability of angiography and venography will benefit from quantitative analysis/postprocessing

Measures of interest:

- Both arteries and veins:
  Vessel density, - length, - tortuosity, - branching patterns (nr of branches or fractal dimension)
- Arteries only:
  Vessel diameters, total vessel volume
- Veins only:
  Oxygenation levels (quantitative susceptibility mapping)

Strategy for obtaining normative data on these measures:

- Optimize and harmonize TOF [6] and SWI protocols across sites
- Develop and implement automated image analysis (user supervision/censoring allowed)
  - Automated arterial segmentation [7]
  - Automated venous segmentation [8]
  - Automated measures as listed above from segmented vessels [9] [10]
- Motion remains a challenge for for longer term

Vessel wall

- 7T (and 3T) MRI allows for imaging of intracranial vessel walls (reviews: [11] [12])
- Still limited to larger vessels (circle of Willis and a few major branches)
- Still of interest for studying relation between dementia and vascular disease; predominantly for (lacunar) infarctions and cerebral amyloid angiopathy

Measures of interest:

- Vessel wall lesions, enhancing or non-enhancing
- Vessel wall thickness
- Vessel wall stiffness

Strategy for obtaining normative data on these measures:

- Optimize and harmonize protocols: choice for CSF suppression approach not established yet
- Develop automated/objective rating of images (vessel wall thickness, and enhancement of lesions)

Vessel function

- Blood flow
- Effective damping of pulsations towards small vessels, assessable by looking at velocity pulsation in small penetrating arteries [13] [14]
- Vascular reactivity to CO2 or neuronal stimulation
- Blood-brain-barrier integrity; Can be partially assessed by looking to contrast agent leakage [15] and possibly also by looking to water transport across the BBB [ref to S. Schmid & Thijs van Osch]

Measures of interest:

- Blood flow: relative contributions from major vessels circle of Willis, and draining veins
- Damping: Pulsatility index
- Reactivity: BOLD, flow, diameter and/or velocity change upon standardized challenge (CO2 or basic functional stimulus like visual checkerboard fMRI).
- BBB: k_{trans}, obtained from dynamic susceptibility contrast [DSC] MRI and dynamic contrast enhancement [DCE] MRI
- BBB: Water transport flux

Strategy for obtaining normative data on these measures:

- Blood flow: 4D PCA
- Pulsatility index: harmonize protocols (4D PCA for larger vessels? + 2D PCA for penetrating arteries).
- Ktrans: protocol optimization
- Water transport flux: needs further validation at 3T, and translation to 7T (similar challenges as ASL)

Cerebral blood flow

- *Measures of interest:*

- Regional CBF
- Mean arterial transit times
- Regional blood volume

Strategy for obtaining normative data on these measures

- Still technological developments needed for robust ASL with whole brain coverage at 7T (proper labeling coil is needed; RF homogeneity needs to be controlled).

Vascular Lesions

- Microinfarcts [16] [17] [18]
- Microbleeds [19] [20]
- Focal atrophy/secondary [21] neurodegeneration

Results from the EUFIND 2D phase contrast imaging in perforating arteries

This report briefly describes the results from the preliminary analysis of the 2D phase contrast data obtained from 2 subjects per site in the EUFIND multi-center-study. (For details of the Methods, including planning and the scan parameters per vendor, see the 'EUFIND - SOP 2D phase contrast perforating arteries - version 2.docx').

Analysis

The analysis was performed by the UMC Utrecht with custom built Matlab code that has been previously described [22, 23]. In brief: First, a manual region of interest was drawn to delineate the basal ganglia. Background phase errors were removed using a median filter. Next, the standard deviation of the magnitude over the cardiac cycle was used as an estimate of the noise, after which all voxels with a velocity significantly different from the noise level were selected. As the perforating arteries are small, only one voxel with the highest mean velocity was selected from clusters of connected voxels with significant velocity. Finally, voxels with significant velocity that were hyperintense on the magnitude were taken as perforating arteries. Perforators closer than about 0.6 mm were taken as one perforator (taking the one with the highest mean velocity) to avoid multiple detections of perforators that were oblique to the imaged plane. For each subject, the number of detected perforators, their mean velocity and the pulsatility index of the average velocity curve (over all detected perforators) were recorded.

Changed slice planning

The initial aim was to apply the 2D phase contrast to the perforating arteries of the white matter in the semioval center. However, initial results from sites with a different vendor than the vendor for which the sequence was developed, showed no detectable perforating arteries (n=7 subjects). The different performance of this method at different vendors is not yet understood, and illustrates the need and challenge for harmonization. As a fallback, the 2D phase contrast scan was applied to the perforating arteries in the basal ganglia (BG), which are easier to detect, due to diameters and faster blood flow compared to the perforating arteries in the white matter.

Results and Discussion

Eleven 2D phase contrast scans in the BG were available from 7 sites (Copenhagen, Essen, Leipzig, Magdeburg, Pisa, Oxford, Utrecht). All 11 datasets could be successfully analyzed, after

some minor adjustments to the code to allow correct reading of the data with variable DICOM headers. The number of detected perforators was (average ± standard deviation): 22 ± 12 (range 6-39). The mean velocity was 4.3 ± 1.3 cm/s, and the pulsatility index was 0.34 ± 0.13.

The results match well with the values from the first publication where the method was applied in 6 relatively young subjects (age range: 23-29) [23]. In that study, 16 ± 8 vessels were found, but those were manually selected with the additional requirement that the vessels were visible in two repeated scans. The mean velocity and pulsatility index in that study were 4.6 ± 0.5 cm/s and 0.44 ± 0.07 respectively, which compares well with the values found in the current study. The larger standard deviations in the current study might reflect inter-site variability, but may also be partly due to a difference in age of the participants. Further improvement of the analysis tool is needed to deal with perforating arteries that are not perpendicular to the plane, and run for a considerable distance in-plane in the imaged slice, as those yield sometimes multiple detected perforators by the current semi-automatic detection algorithm.

References

1. Stroke. 2017 Nov;48(11):3175-3182. doi: 10.1161/STROKEAHA.117.016996. Epub 2017 Sep 29.*Targeting Cerebral Small Vessel Disease With MRI*. Zwanenburg JJM1, van Osch MJP2. PMID: 28970280.
2. Different types of white matter hyperintensities in CADASIL: Insights from 7-Tesla MRI. De Guio F, Vignaud A, Chabriat H, Jouvent E.J Cereb Blood Flow Metab. 2017 Jan 1:271678X17690164. doi: 10.1177/0271678X17690164. [Epub ahead of print] PMID: 28128022.
3. Non-enhanced magnetic resonance imaging of unruptured intracranial aneurysms at 7 Tesla: Comparison with digital subtraction angiography.Wrede KH, Matsushige T, Goericke SL, Chen B, Umutlu L, Quick HH, Ladd ME, Johst S, Forsting M, Sure U, Schlamann M.Eur Radiol. 2017 Jan;27(1):354-364. Epub 2016 Mar 18.PMID:26993650.
4. MR venography of the human brain using susceptibility weighted imaging at very high field strength. Koopmans PJ, Manniesing R, Niessen WJ, Viergever MA, Barth M.MAGMA. 2008 Mar;21(1-2):149-58. doi: 10.1007/s10334-007-0101-3. Epub 2008 Jan 11.
5. Loss of venous integrity in cerebral small vessel disease: a 7-T MRI study in cerebral autosomal-dominant arteriopathy with subcortical infarcts and leukoencephalopathy (CADASIL). De Guio F, Vignaud A, Ropele S, Duering M, Duchesnay E, Chabriat H, Jouvent E. Stroke. 2014 Jul;45(7):2124-6. doi: 10.1161/STROKEAHA.114.005726. Epub 2014 May 27. PMID: 24867926.
6. The traveling heads: multicenter brain imaging at 7 Tesla. Voelker MN, Kraff O, Brenner D, Wollrab A, Weinberger O, Berger MC, Robinson S, Bogner W, Wiggins C, Trampel R, Stöcker T, Niendorf T, Quick HH, Norris DG, Ladd ME, Speck O. MAGMA. 2016 Jun;29(3):399-415. doi: 10.1007/s10334-016-0541-8. Epub 2016 Apr 20. PMID: 27097904.
7. Radbruch A, et al. Quantification of tumor vessels in glioblastoma patients using time-offlight angiography at 7 Tesla: a feasibility study. PLoS One. 2014 Nov 21;9(11):e110727.
8. Monti S, et al. MAVEN: an Algorithm for Multi-Parametric Automated Segmentation of Brain Veins from Gradient Echo Acquisitions. IEEE Trans Med Imaging 2017 May; 36(5):1054-1065.
9. Abnormalities of Cerebral Deep Medullary Veins on 7 Tesla MRI in Amnestic Mild Cognitive Impairment and Early Alzheimer's Disease: A Pilot Study. Bouvy WH, Kuijf HJ, Zwanenburg

JJ, Koek HL, Kappelle LJ, Luijten PR, Ikram MK, Biessels GJ; Utrecht Vascular Cognitive Impairment (VCI) Study group. J Alzheimers Dis. 2017;57(3):705-710. doi: 10.3233/JAD-160952. PMID: 28282806.

10. Quantification of deep medullary veins at 7 T brain MRI. Kuijf HJ, Bouvy WH, Zwanenburg JJ, Razoux Schultz TB, Viergever MA, Vincken KL, Biessels GJ. Eur Radiol. 2016 Oct;26(10):3412-8. doi: 10.1007/s00330-016-4220-y. Epub 2016 Feb 16. PMID: 26883328.
11. Stroke. 2017 Nov;48(11):3175-3182. doi: 10.1161/STROKEAHA.117.016996. Epub 2017 Sep 29.Targeting Cerebral Small Vessel Disease With MRI.Zwanenburg JJM1, van Osch MJP2.
12. Dieleman,N, van der Kolk,AG, Zwanenburg,JJ, Harteveld,AA, Biessels,GJ, Luijten,PR, Hendrikse,J: Imaging intracranial vessel wall pathology with magnetic resonance imaging: current prospects and future directions. Circulation 130:192-201, 2014.
13. Better and faster velocity pulsatility assessment in cerebral white matter perforating arteries with 7T quantitative flow MRI through improved slice profile, acquisition scheme, and postprocessing. Geurts L, Biessels GJ, Luijten P, Zwanenburg J. Magn Reson Med. 2017 Jul 11. doi: 10.1002/mrm.26821. [Epub ahead of print]. PMID:28699211.
14. Assessment of blood flow velocity and pulsatility in cerebral perforating arteries with 7-T quantitative flow MRI. Bouvy WH, Geurts LJ, Kuijf HJ, Luijten PR, Kappelle LJ, Biessels GJ, Zwanenburg JJ.NMR Biomed. 2016 Sep;29(9):1295-304. doi: 10.1002/nbm.3306. Epub 2015 Apr 27. PMID:25916399.
15. Assessment of blood-brain barrier disruption using dynamic contrast-enhanced MRI. A systematic review. Heye AK, Culling RD, Valdés Hernández Mdel C, Thrippleton MJ, Wardlaw JM. Neuroimage Clin. 2014 Sep 10;6:262-74. doi: 10.1016/j.nicl.2014.09.002. eCollection 2014. Review.PMID: 25379439.
16. Intracortical infarcts in small vessel disease: a combined 7-T postmortem MRI and neuropathological case study in cerebral autosomal-dominant arteriopathy with subcortical infarcts and leukoencephalopathy. Jouvent E, Poupon C, Gray F, Paquet C, Mangin JF, Le Bihan D, Chabriat H. Stroke. 2011 Mar;42(3):e27-30. doi: 10.1161/STROKEAHA.110.594218. Epub 2011 Feb 3.PMID:21293025.
17. Detection, risk factors, and functional consequences of cerebral microinfarcts. van Veluw SJ, Shih AY, Smith EE, Chen C, Schneider JA, Wardlaw JM, Greenberg SM, Biessels GJ.Lancet Neurol. 2017 Sep;16(9):730-740. doi: 10.1016/S1474-4422(17)30196-5. Epub 2017 Jul 14. Review. PMID: 28716371.
18. In vivo detection of cerebral cortical microinfarcts with high-resolution 7T MRI. van Veluw SJ, Zwanenburg JJ, Engelen-Lee J, Spliet WG, Hendrikse J, Luijten PR, Biessels GJ.J Cereb Blood Flow Metab. 2013 Mar;33(3):322-9. doi: 10.1038/jcbfm.2012.196. Epub 2012 Dec 19.PMID: 23250109.
19. Cerebral microbleeds on MR imaging: comparison between 1.5 and 7T. Conijn MM, Geerlings MI, Biessels GJ, Takahara T, Witkamp TD, Zwanenburg JJ, Luijten PR, Hendrikse J. AJNR Am J Neuroradiol. 2011 Jun-Jul;32(6):1043-9. doi: 10.3174/ajnr.A2450. Epub 2011 May 5.PMID: 21546463.
20. Efficient detection of cerebral microbleeds on 7.0 T MR images using the radial symmetry transform. Kuijf HJ, de Bresser J, Geerlings MI, Conijn MM, Viergever MA, Biessels GJ, Vincken KL.Neuroimage. 2012 Feb 1;59(3):2266-73. doi: 10.1016/j.neuroimage.2011.09.061. Epub 2011 Oct 2. PMID: 21985903.
21. In vivo high-resolution 7 Tesla MRI shows early and diffuse cortical alterations in CADASIL. De Guio F, Reyes S, Vignaud A, Duering M, Ropele S, Duchesnay E, Chabriat H, Jouvent

E. PLoS One. 2014 Aug 28;9(8):e106311. doi: 10.1371/journal.pone.0106311. eCollection 2014. PMID:25165824.

22. Geurts L, Biessels GJ, Luijten P, and Zwanenburg J, Better and faster velocity pulsatility assessment in cerebral white matter perforating arteries with 7T quantitative flow MRI through improved slice profile, acquisition scheme, and postprocessing. Magn Reson Med, 2017.
23. Bouvy WH, Geurts LJ, Kuijf HJ, Luijten PR, Kappelle LJ, Biessels GJ, and Zwanenburg JJ, *Assessment of blood flow velocity and pulsatility in cerebral perforating arteries with 7-T quantitative flow MRI.* NMR Biomed, 2016. **29**(9): p. 1295-304.

Subgroup contributors

Geert Jan Biessels, Hugues Chabriat, Mauro Costagli, Martin Dichgans, Emrah Duzel, Francois De Guio, Susan Francis, Eric Jouvent, Jeroen Hendrikse, Oliver Kraff, Mark Ladd, Harald Moeller, Armin Nagel, Harald Quick, Esben Thade Petersen, Matthias Schroeter, Oliver Speck, Kamil Uludag, Marc von Buchem, Maxim Terekhov, Laura Schreiber, Alexandre Vignaud, Arno Villringer, Joanna Wardlaw, Richard Wise, Jaco Zwanenburg

E. Macromolecular pathology

***Subgroup coordinators**: Julio Acosta-Cabronero, Richard Bowtell*

Iron dysregulation is thought to play a relevant role in the pathogenesis of neurodegenerative diseases such as Parkinson's disease[1], Wilson's disease[2], amyotrophic lateral sclerosis[3] or Alzheimer's disease[4]. At present, however, it is unclear whether iron-mediated mechanisms are a primary cause or a secondary consequence of neurodegeneration[5] [6]. Mapping the spatial distribution and temporal dynamics of iron deposition may offer important insights, and if sufficiently robust, it could even offer a disease-monitoring tool.

Quantitative susceptibility mapping (QSM) and measurement of the apparent transverse relaxation rate (R_2*) are the most commonly used MRI approaches for mapping brain iron in vivo[7]. Although neither measure is exclusively modulated by iron concentration – they are also sensitive to e.g. myelin and calcium content – post-mortem investigations have shown that variation in iron content is the dominant cause of variation of susceptibility and R_2* in several brain structures, including most deep brain nuclei and cortex[8-12]. Besides, on post-mortem examination, intriguingly large numbers of iron-laden glial cells have been identified in the vicinity of pathological inclusions in all the major neurodegenerative diseases[13-15]; and 3T QSM investigations are also emerging, which reveal highly specific patterns—suggestive of iron accumulation—in aging[16] and neurodegenerative diseases[17] [18]. Thus, new in vivo iron mapping developments aiming at greater sensitivity and stability might offer important pathomechanistic clues in neurodegenerative diseases, beyond our current understanding based on the characterisation and distribution of histopathological inclusions in each of these diseases[19-21].

The advent of ultra-high field (UHF) MRI opens a new window of opportunity for QSM and R_2* measurements. Both measures are largely driven by a fundamental electromagnetic property, namely magnetic susceptibility; and notably, the effects on the MRI signal due to tissue susceptibility differences are greatly amplified at UHF. This is because field inductions leading to spin dephasing, and thus contrast differences, are linearly related to field strength.

At present, we lack conclusive evidence for the unique value of QSM or R_2* as imaging biomarkers at UHF, or at least their value over and above the potential they have shown at 3T. However, early 7T results[22] suggest the greater sensitivity and higher image resolutions achievable at high field might result in a more pro-active role for MRI in neurodegenerative pathology detection and disease monitoring. While this might be true, several technical challenges are still unresolved, most of which could have a detrimental impact on measurement stability. In such context, the EUFIND consortium has agreed to carry out a systematic calibration of QSM and R_2* estimates from multiple sites (using scanners from three different manufacturers) with the view to enable susceptibility and R_2* mapping for large-scale research studies and clinical trials at 7T – the first study of this kind at high field.

Methods

Two, 3D spoiled gradient-echo (FLASH) sequences were optimised for three scanner types (Siemens, Philips and General Electric). The rationale was to have all sites acquire a whole-brain, high in-plane resolution, fully flow-compensated scan under 10 minutes with potential to map neurodegenerative disease and vascular pathology in single subjects with susceptibility MRI; and at some sites, in addition, acquire a multi-echo set (also under 10 mins) for simultaneous sub-millimetre QSM/R_2* quantification. Scan details are summarised in the tables at the end of this section.

Multi-vendor data from n=12 subjects acquired at six different sites were preliminarily investigated to work out the logistics for data management, reconstruction and analysis, and to try to identify at a sufficiently early stage whether any major inconsistencies in data acquisition or format exist. DICOM data, saved uncombined for Siemens acquisitions or coil-combined (with scanner software) for Philips and GE data, were uploaded from each site to a centrally managed XNAT server (https://www.xnat.org). Notably, to date (22/11/2017), datasets from thirteen sites have been successfully uploaded. Multi-coil single-echo Siemens data sets were reconstructed as follows: 3D phase maps from each coil element were separately unwrapped with a discrete Laplacian method[23] and were background filtered using a two-step harmonic-estimation procedure consisting of Laplacian boundary value[24] and variable spherical mean value methods[25]; the latter using an initial kernel radius of 25 mm. Such pre-processing removes any coil-specific phase offsets, thus robust coil-combination for Siemens data could be achieved with a simple magnitude-square weighted filtered-phase sum. The same unwrapping and two-step background extraction algorithms were used for combined Philips and GE data prior to inversion with a recently developed multi-scale (nonlinear MEDI[26] based) approach (in submission). The regularisation parameter was preliminarily optimised for a single (Siemens) dataset with the L-curve method[27]. In addition, multi-echo data from n=6 subjects (two from Philips, three from Siemens and one from a GE system) were processed as described elsewhere[28]. Prior to this, in order to harmonise data input across vendors, Siemens data underwent a coil-combination step using the phase distribution of the first echo as a reference. In addition, the linear phase adjustment enforced by the Philips reconstruction software was removed. Briefly, the subsequent processing steps for multi-echo data consisted of a non-linear least-squares fitting of magnitude data to an exponential decay for T_2* estimation, and a QSM reconstruction pipeline with the following steps: field map calculation based on a non-linear temporal fitting of the complex signal, brain mask extraction[29] from the magnitude data of the first echo, background field removal using the projection onto dipole fields method[30] and QSM inversion using MEDI[31]. All parameter maps were finally converted to DICOM format, updated to the XNAT database for centralised review, and were subsequently spatially standardised to ease comparability with a previously optimised co-registration routine[16].

Results

QSM reconstructions were performed successfully for all twelve single-echo datasets (Fig. 1). Independently, i.e. with a different pipeline implemented at a different site[28], n=6 multi-echo sets were also successfully processed (Fig. 2, only n=4 sets shown). On visual inspection, n=4 (out of 12) single-echo and n=2 (out of 6) multi-echo scans were moderately corrupted by subject motion, from which two datasets (one for each scan type) were deemed to be “possibly unusable”. At this early stage, QSM variability appears to be relatively high across scanner vendors, or at least higher than for Siemens-only reconstructions (Fig. 3). However, a simple exercise focusing on the striatum (with the prediction that QSM should be increased as a function of age[16]) returned a qualitatively positive result (Fig. 4).

Conclusions

We have demonstrated QSM and R_2* can be reliably reconstructed from 7T scans acquired at different sites using different scanner types. Notably, participation was high with most site representatives either interested or actively participating in this particular arm of the project. Consequently, custom solutions for data storage, management and processing had to be identified, developed and deployed within EUFIND’s collaborative framework. At the next stage (i.e. through a pilot study where n=10 datasets from elderly individuals will be acquired at most

EUFIND sites), we will be able to address systematically highly relevant questions ranging from technical aspects, largely aiming at characterising QSM/R_2* stability, to applications, where we will be able to calibrate the potential of both techniques to detect aging and disease related alterations.

Siemens protocol

Sequence	3D single-echo FLASH	3D multi-echo FLASH [*24-channel head coil]
FOV, mm	224×196×150	224×196×157
Matrix dimensions	640×560×120	320×280×224
Voxel size, mm	0.35×0.35×1.25	0.7×0.7×0.7
Flip angle, deg	10 ($T_{1,\ Ernst}$=1200 ms)	15 ($T_{1,\ Ernst}$=800 ms)
Flow compensation	3D	3D, first echo only
TE, ms	10	5.3, 11.5, 17.8, 24.0 [*5.3, 9.0, 12.8, 16.5, 20.3, 24.0] unipolar readouts
Bandwidth, Hz/px/echo	100	430 [*360]
RF spoiling	On	On
Partial Fourier	7/8 (phase), 7/8 (slice)	7/8 (slice)
GRAPPA (factor, ref lines)	2 (phase), 32	4 (phase), 40
TR, ms	18	27
Oversampling, mm	10 (slice)	11.2 (slice)
TA, min	8:46	9:23

Philips protocol

Sequence	3D single-echo FLASH	3D multi-echo FLASH
FOV, mm	224×192×150	224×196×157
Matrix dimensions	ACQ (640×547×120) REC (672×672×120)	ACQ (320×280×224) REC (320 x 320 x 224)
Voxel size, mm	0.35×0.35×1.25	0.7×0.7×0.7
Flip angle, deg	10	15
Flow compensation	3D	3D, first echo only
TE, ms	10	5.25, 9.0, 12.75, 16.5, 20.25, 24.0 unipolar readouts
Bandwidth, Hz/px/echo	101	429
RF spoiling	On	On
Partial Fourier	No	No
SENSE factor (RL x FH)	2.1 x 1	2 x 2
TR, ms	18	27
Oversampling factor	1.07 (slice)	1.07 (slice)
TA, min	7:50	9:24

GE protocol

Sequence	3D single-echo FLASH	3D multi-echo FLASH
FOV, mm	205×172×144	192×192×150
Matrix dimensions	512×430×120	320×280×224
Voxel size, mm	0.4×0.4×1.2	0.7×0.7×0.7
Flip angle, deg	10	15
Flow compensation	On	On (slice)
TE, ms	9.7	5.6, 9.5, 13.4, 17.3, 21.2, 25.1, 29.0, 32.9, 36.8, 40.7 bipolar readouts
Bandwidth, Hz/px/echo	98	456
RF spoiling	On	On
Partial Fourier	No	0.77
ASSET factor	2 (phase)	3 (phase)
TR, ms	18.5	44
Oversampling, mm	-	-
TA, min	7:59	8:50

References

1. Sian-Huelsmann J, Mandel S, Youdim MB, et al. *The relevance of iron in the pathogenesis of Parkinson's disease.* J Neurochem 2011;118(6):939-57. doi: 10.1111/j.1471-4159.2010.07132.x
2. Dusek P, Roos PM, Litwin T, et al. *The neurotoxicity of iron, copper and manganese in Parkinson's and Wilson's diseases.* J Trace Elem Med Biol 2015;31:193-203. doi: 10.1016/j.jtemb.2014.05.007
3. Lovejoy DB, Guillemin GJ. *The potential for transition metal-mediated neurodegeneration in amyotrophic lateral sclerosis*. Front Aging Neurosci 2014;6:173. doi: 10.3389/fnagi.2014.00173
4. Smith MA, Harris PL, Sayre LM, et al. *Iron accumulation in Alzheimer disease is a source of redox-generated free radicals*. Proc Natl Acad Sci U S A 1997;94(18):9866-8.
5. Zecca L, Youdim MB, Riederer P, et al. *Iron, brain ageing and neurodegenerative disorders*. Nat Rev Neurosci 2004;5(11):863-73. doi: 10.1038/nrn1537
6. Ke Y, Ming Qian Z. *Iron misregulation in the brain: a primary cause of neurodegenerative disorders.* Lancet Neurol 2003;2(4):246-53.
7. Betts MJ, Acosta-Cabronero J, Cardenas-Blanco A, et al. *High-resolution characterisation of the aging brain using simultaneous quantitative susceptibility mapping (QSM) and R2* measurements at 7T.* Neuroimage 2016;138:43-63. doi: 10.1016/j.neuroimage.2016.05.024
8. Langkammer C, Schweser F, Krebs N, et al. *Quantitative susceptibility mapping (QSM) as a means to measure brain iron? A post mortem validation study*. Neuroimage 2012;62(3):1593-9. doi: 10.1016/j.neuroimage.2012.05.049

9. Sun H, Walsh AJ, Lebel RM, et al. *Validation of quantitative susceptibility mapping with Perls' iron staining for subcortical gray matter.* Neuroimage 2015;105:486-92. doi: 10.1016/j.neuroimage.2014.11.010
10. Zheng W, Nichol H, Liu S, et al. *Measuring iron in the brain using quantitative susceptibility mapping and X-ray fluorescence imaging*. Neuroimage 2013;78:68-74. doi: 10.1016/j.neuroimage.2013.04.022
11. Fukunaga M, Li TQ, van Gelderen P, et al. *Layer-specific variation of iron content in cerebral cortex as a source of MRI contrast.* Proc Natl Acad Sci U S A 2010;107(8):3834-9. doi: 10.1073/pnas.0911177107
12. Langkammer C, Krebs N, Goessler W, et al. *Quantitative MR imaging of brain iron: a postmortem validation study*. Radiology 2010;257(2):455-62. doi: 10.1148/radiol.10100495
13. Connor JR, Snyder BS, Beard JL, et al. *Regional distribution of iron and iron-regulatory proteins in the brain in aging and Alzheimer's disease*. J Neurosci Res 1992;31(2):327-35. doi: 10.1002/jnr.490310214
14. Kwan JY, Jeong SY, Van Gelderen P, et al. *Iron accumulation in deep cortical layers accounts for MRI signal abnormalities in ALS: correlating 7 tesla MRI and pathology*. PLoS One 2012;7(4):e35241. doi: 10.1371/journal.pone.0035241
15. McGeer PL, Itagaki S, Akiyama H, et al. *Rate of cell death in parkinsonism indicates active neuropathological process.* Ann Neurol 1988;24(4):574-6. doi: 10.1002/ana.410240415
16. Acosta-Cabronero J, Betts MJ, Cardenas-Blanco A, et al. *In Vivo MRI mapping of brain iron deposition across the adult lifespan.* J Neurosci 2016;36(2):364-74. doi: 10.1523/JNEUROSCI.1907-15.2016
17. Acosta-Cabronero J, Cardenas-Blanco A, Betts MJ, et al. T*he whole-brain pattern of magnetic susceptibility perturbations in Parkinson's disease*. Brain 2017;140(Pt 1):118-31. doi: 10.1093/brain/aww278
18. Acosta-Cabronero J, Williams GB, Cardenas-Blanco A, et al. *In vivo quantitative susceptibility mapping (QSM) in Alzheimer's disease*. PLoS One 2013;8(11):e81093. doi: 10.1371/journal.pone.0081093
19. Braak H, Ghebremedhin E, Rub U, et al. *Stages in the development of Parkinson's disease-related pathology*. Cell Tissue Res 2004;318(1):121-34. doi: 10.1007/s00441-004-0956-9
20. Braak H, Braak E. N*europathological stageing of Alzheimer-related changes.* Acta Neuropathol 1991;82(4):239-59.
21. Brettschneider J, Del Tredici K, Toledo JB, et al. *Stages of pTDP-43 pathology in amyotrophic lateral sclerosis.* Ann Neurol 2013;74(1):20-38. doi: 10.1002/ana.23937
22. Dusek P, Skoloudik D, Maskova J, et al. *Brain iron accumulation in Wilson's disease: A longitudinal imaging case study during anticopper treatment using 7.0T MRI and transcranial sonography.* J Magn Reson Imaging 2017 doi: 10.1002/jmri.25702
23. Schofield MA, Zhu Y. *Fast phase unwrapping algorithm for interferometric applications*. Opt Lett 2003;28(14):1194-6.
24. Zhou D, Liu T, Spincemaille P, et al. *Background field removal by solving the Laplacian boundary value problem*. NMR Biomed 2014;27(3):312-9. doi: 10.1002/nbm.3064
25. Li W, Wu B, Liu C. *Quantitative susceptibility mapping of human brain reflects spatial variation in tissue composition.* Neuroimage 2011;55(4):1645-56. doi: 10.1016/j.neuroimage.2010.11.088
26. Liu T, Wisnieff C, Lou M, et al. *Nonlinear formulation of the magnetic field to source relationship for robust quantitative susceptibility mapping*. Magn Reson Med 2013;69(2):467-76. doi: 10.1002/mrm.24272

27. Hansen P, O'Leary D. *The use of the L-curve in the regularization of discrete ill-posed problems.* SIAM J Sci Comput 1993;14(6):1487-503. doi: 10.1137/0914086
28. De Rochefort L, Girard O, Le Troter A, et al. *Clinical brain QSM acquisition and automated processing at 3 and 7 T for routine use*. Proc ESMRMB 2017:446.
29. Smith SM. *Fast robust automated brain extraction*. Hum Brain Mapp 2002;17(3):143-55.
30. Liu T, Khalidov I, de Rochefort L, et al. A *novel background field removal method for MRI using projection onto dipole fields* (PDF). NMR Biomed 2011;24(9):1129-36. doi: 10.1002/nbm.1670
31. Liu T, Liu J, de Rochefort L, et al. *Morphology enabled dipole inversion (MEDI) from a single-angle acquisition: comparison with COSMOS in human brain imaging*. Magn Reson Med 2011;66(3):777-83. doi: 10.1002/mrm.22816

Subgroup contributors

Richard Bowtell; Peter Nestor; Julio Acosta-Cabronero; Rochefort de Ludovic; Harald Moeller; Mauro Costagli; Esben Thade Petersen; Cyril Poupon; Tony Stöcker; Kamil Uludag; Nikolaus Weiskopf; Mark Ladd

F. Spectroscopy

Subgroup coordinators: *Ariane Fillmer, Florian Schubert, Penny Gowland, Itamar Ronen*

In vivo MR spectroscopy (MRS) (1) and CEST spectroscopy (2) are the only methods that are capable of noninvasively quantifying a portion of the biochemical composition of living tissue, either directly or via saturation transfer. Of these techniques, proton (^{1}H) MRS has reached the arena of clinical research both due to its ability to detect and quantify a fair number of relevant metabolites in human brain in vivo, and because appropriate sequences are available, in principle, on every clinical MR scanner.

Proton MRS

^{1}H MRS has been used in neurodegenerative disease (NDD) research in both cross sectional and longitudinal investigations, in order to elucidate possible correlations of brain metabolites with cognition, body fluid biomarkers of NDD and the course of treatment strategies. Altered neurometabolic profiles have been detected in MCI and AD using ^{1}H MRS, but no definitive biomarker(s) of MCI or AD have been established so far. There is clear evidence for the neuron marker N-acetylaspartate (NAA) to be reduced and glial marker myo-inositol (Ins) to be enhanced in AD as compared to MCI and healthy aged brain (see (3) for a meta-analysis). At B_0 up to 3 T, where the relatively strong resonances of NAA, total creatine (tCr), total choline (tCho) and myo-inositol (Ins) can be estimated quite well, the role of NAA and Ins in MCI and AD has been firmly established. However, up to now mostly metabolite ratios are given for the inability to obtain a true quantification at these field strengths. Thus, Ins/NAA has been shown among the metabolite ratios to be the strongest predictor for AD, and the ability of MRS to distinguish AD patients from controls was reflected by sensitivities between 57 % and 90 % and specificities between 73 % and 95 %, depending on the anatomical region analyzed (4). Dealing with memory, visu-spatial functions and language, the posterior cingulate cortex (PCC) appears to be among the regions to reflect the earliest MRS-related signs of abnormalities. NAA/tCr in PCC has been shown to differentiate between controls, AD and amnestic MCI patients (5), and to differentially predict conversion from MCI to AD and Lewy Body Dementia (6). There is additional evidence that β-amyloid (Abeta) load is associated with MRS-quantifiable abnormalities in cognitively normal older subjects. MRS at 3 T has established correlations between brain Abeta and Ins/tCr and tCho/tCr in PCC of aging adults (5, 6) and between NAA/tCr and CSF Abeta and Tau in AD patients (7). NAA/tCr and Ins/tCr also correlate with cognition scores, memory, hippocampal volume and resting state fMRI in aged healthy controls (4). Higher magnetic field (3 and 4 T) provided first evidence of diminished neurotransmitter glutamate (8, 9) and GABA (10). Glutathione (GSH, an oxidative stress protector) was correlated with cognitive functions and discriminated between controls and MCI and, less clearly, AD patients (11).

Findings for Parkinson's disease appear to have a focus on the reduction of NAA as a neuronal marker. Decreased glutamate + glutamine has also been observed, namely in the lentiform nucleus of Parkinson's patients (12), whereas studies at 7 T revealed increased GABA levels in pons and putamen (13) and a therapeutic enhancing effect of N-acetylcysteine on GSH concentration in occipital cortex (14).

Thus, ^{1}H MRS may provide predictive information complementary to body fluid biomarkers and is particularly valuable at early stages of NDD prior to detectable morphometric changes. However, a more specific metabolic picture can only be achieved when, in addition to the above compounds, glutamine and glutamate can be reliably separated, and low-level metabolites (0.5-3 mmol/l), such as GABA, glutamine and GSH, will become accessible to a quantitative

measurement with acceptable imprecision, i.e. uncertainties below 10 %. Likewise, treatment evaluation studies using MRS, having been carried out with mixed results at lower field strengths, will benefit from a comprehensive knowledge of the evolution of more metabolite concentrations over time (1).

It is therefore of high importance to quantify these metabolites with higher accuracy and establish the uncertainties of the spectral fitting procedures used to enhance their diagnostic accuracy. In contrast to the limitations of $B_0 \leq 3$ T regarding SNR and spectral dispersion, MRS at 7 T will enhance the sensitivity and spectral resolution and enable neurochemical profiles to be quantified with up to 17 metabolites (15), thus permitting high accuracy for the above singlets and the quantification of neurotransmitters like glutamate, GABA, aspartate and glutamine, but also GSH, with good precision. For this purpose, semi-LASER appears to be the sequence of choice as it combines reasonably short echo times with relatively low chemical shift displacement artifact, and has been applied at 7 T sites using different vendors (16). In order to exploit all these benefits of 7 T, one of the most important challenges is certainly the increased inhomogeneity induced by the subject itself at increased field strengths (17). The need to overcome these inhomogeneities, especially for MRS applications (but equally important for X-nuclei MRS and CEST), recently inspired the development of more sophisticated so-called B_0-shimming techniques for ultra-high field applications (e.g. 18 - 20) than are necessary at lower field strengths.

Most studies of MR spectroscopy in NDDs focus on a single region of interest, so far. However, magnetic resonance spectroscopic imaging (MRSI) (21) does offer the possibility in observing the spatial distribution of changes in the neurochemical profiles. This becomes increasingly interesting at 7T, as the increased field strength helps to overcome the intrinsically limited SNR associated with this method and recently developed techniques improve the spatial specificity of MRSI (22, 23), in order to improve robustness of quantification.

An additional analytical dimension is added to MRS by diffusion weighting, which allows insight into compartment specific and cell-preferential tissue properties and their evolution on a cytomorphological level. This technique allows for the investigation of the apparent diffusion coefficients (ADCs) of the brain metabolites, an effective diffusivity that depends on a number of factors that influence the random motion of the metabolites in the intracellular and extracellular compartments (24), e.g. specific binding of metabolites to cell structures, and dimensions of intervening immobile structures.

Diffusion properties of neuronal and glial metabolites measured at 7T have contributed to the explanation of pathological processes in multiple sclerosis (MS) and in neuropsychiatric systemic lupus erythematosus (NPSLE): in MS, the cytosolic diffusivity of tNAA (the sum of NAA and N-Acetylaspartyglutamate, NAAG) has been shown to be a potential putative marker for axonal pathology (25), and the ADC values of tCho correlated well with the inflammatory state of NPSLE patients (26) and may indicate cytomorphological changes in reactive glia. Just as conventional MRS, diffusion weighted MRS (DW-MRS) gains tremendously from the transition to 7T: the increase in SNR with increased field strength results, in a more than linear enhancement in the accuracy of the determined metabolite ADCs, since the error in the calculation of metabolite ADCs propagates non-linearly.

The merits of 7T for conventional MRS as well as DW-MRS will thus underpin application of MRS for early diagnosis of neurodegenerative diseases.

X-nuclei

Targeting other nuclei than protons by MRS, such as ^{31}P and ^{13}C, allows to investigate e.g. different elements of the energy metabolism and, hence, to gain complementary information to ^{1}H MRS.

In AD brain, in vivo ^{31}P MRS has revealed some interesting findings, including alkalinization (as compared to acidification in normal aging) and deviant phosphoester metabolism (27). In Parkinson's disease altered high-energy phosphate levels have been found (28). Furthermore, the possibility of measuring metabolic fluxes using e.g. magnetization transfer spectroscopic measurements (29) holds significant promise for X-nuclei measurements in neurodegenerative disorders such as Huntington's disease, where cortical metabolic deficits have been detected in premanifest patients (30), which were partially reversed by treatment with Triheptanoin (31).
Contrary to ^{1}H MRS, however, this technique has not found widespread application due to technical limitations, such as the need for additional hardware. Nevertheless, X-nuclei MRS gains significantly from the transition to 7T in much of the same ways as ^{1}H MRS does. Moreover, since their resonance frequencies are lower than that of ^{1}H, the gains in sensitivity are not countered by the adverse effects of strongly inhomogeneous B_1, as encountered in ^{1}H MRS. Hence, X-nuclei MRS at 7T is a valuable research tool, which will help to better understand underlying processes in NDDs, and therefore, leading to earlier diagnosis as well as better treatment.

CEST imaging

Chemical exchange saturation transfer (CEST) imaging is a relatively new technique that can provide metabolic information with high sensitivity, but currently with low specificity compared to MRS (32). The high sensitivity of CEST arises from the fact that the signal from moieties of interest are detected indirectly via the water signal providing sufficient amplification of signal to enable MRI mapping to be performed. Its current lack of specificity originates in signals from different moieties, which overlap and combine in a nonlinear fashion that is acutely dependent on the exact environment (e.g. pH and temperature) and experimental conditions (e.g. field strength). The CEST phenomenon is very closely related to magnetization transfer and requires off-resonance saturation at a range of different frequencies in turn to create a z-spectrum. Broadly there are two ways of acquiring a CEST image. The first one involves interleaving the saturation between each readout pulse of a standard gradient echo imaging sequence, while the second one comprises of applying an extended period of saturation prior to the rapid acquisition of all the data required to produce an image. Both methods have advantages in different situations depending on exchange times and other factors (33).
So far, amide proton transfer (APT, CEST of amide protons) has been applied to study tumors, under the assumption that the APT is sensitive to changes in protein synthesis, and thus might be a useful marker of tumor progression (34), and more recently glucose-CEST has been investigated as a method of studying glucose uptake in tumors (35). However, the interpretation of both these results is still under investigation. Furthermore, APT has been used to monitor tissue damage following stroke (36), and glycosaminoglycan- (Gag-)CEST has been used to study connective tissue, in particular cartilage (37). To provide high specificity to particular molecular probes, additionally extrinsic CEST agents have been developed, which so far were only used for animal applications. However, a standard CT agent – iopamidol – also has a CEST affect which can be used to monitor pH, as the exchange processes are often base catalyzed. Finally, the z-spectrum also shows down field features termed nuclear Overhauser effects (NOE), which arise from cross-relaxation and can potentially be used to investigate the three-dimensional structures of abundant macromolecules.
Since CEST imaging is able to target among others concentration differences in macromolecules, like proteins – information that is elusive in MRS – it is capable of offering a wealth of information to complement ^{1}H and X-nuclei MRS techniques. It was demonstrated, for example, that tau pathology in mouse models exhibits changes in gluco-CEST imaging (38). Furthermore, it has been shown that myo-inositol exhibits a CEST effect that can be imaged at ultra-high fields (≥ 7

T) (39). Since it is known that Ins/Cr is altered in e.g. AD, mICEST might provide a tool to investigate disease progression with much higher spatial resolution as the direct detection of Ins by MRS is able to. Moreover, since CEST contrasts are highly dependent on factors like pH, applications in AD patients with alkalinized brain (27) might lead to new insights.
As CEST imaging is still in its infancy, some challenges need to be addressed before it can transition into the clinical routine. Among others, issues regarding quantification and coherent presentation of results, as well as which acquisition methods and analysis approaches can properly address a certain clinical question, need to be resolved.
Just like with MRS, there are great advantages for CEST experiments in transitioning to 7T: the peak separation increases which tends to push molecules into the fast exchange regime, allowing for more robust quantification, and the T1 increases providing increased contrast to noise ratio.

Pilot-Study

Efforts at the Siemens-Sites of the consortium:

While the spectroscopy community of the EUFIND consortium was eager to contribute to the proof-of-concept (PoC) study, several challenges arose. Among them were issues with the sequence homogeneization, pre-measurement calibrations, data formats and post-processing. While in principle a semiLASER sequence was available at all sites, who consented to contribute MR spectroscopy data, the versions of semiLASER are slightly different, allowing for different ranges of sequence parameters, which complicated the process of enabling comparability. Distribution of the same sequence version is complicated by the formal obstacles to be overcome, like legal issues about distribution with Siemens. Overcoming these problems is not impossible, but requires more time than originally expected. Furthermore, pre-measurement calibrations – like B0 shimming and RF calibration – is an issue, that directly influences the data quality, but inbuilt routines at Siemens platforms are not optimized for single voxel spectroscopy measurements, usually leading to rather suboptimal results. Different solutions to this problem are being discussed, for example the distribution of an offline B0 shimming tool, allowing for calculation of optimized B0 shim settings on an additional computer and feeding the results back into the user interface of the scanner. However, distribution of such tools would require easy handling, even for not well experienced users, which still needs to be addressed. Furthermore, the post-processing pipeline in Berlin, where a comparable analysis was supposed to be performed, was not able to read in several data sets. There are several reasons for this, starting with different ways of exporting data from the scanner to different ways data arrays were built, likely due to different sequence versions. Despite all these challenges presented here, the community is eager to further the implementation of comparable routines at different sites for MR spectroscopy, in order to contribute useful data to future works.

Efforts at the GE site of the consortium:

Pisa was the only GE site of the consortium working on acquiring spectroscopy data. In an effort to homogenize the post-processing, GE data were send to Berlin to be processed in the same way as the Siemens data. However, the GE data format for spectroscopy data is very different from the Siemens data format, which made the reading of GE data for the standard tools used in Berlin impossible so far. While the processing tools can certainly be extended with additional read in routines, for now the MR spectroscopy specialist of GE, Dr. Ralf Noeske, agreed to explore the option of conversion routines from GE data format into platform independent data formats.

Efforts at the Philips sites of the consortium:

There are 5 participating Philips sites in the consortium: Utrecht and Leiden (NL), Nottingham (UK), the Danish 7T MRI consortium in Copenhagen (DK) and the Swedish 7T MRI consortium in Lund (SE). Nottingham opted out of the MRS effort and the Swedish consortium data did not arrive to the analyzing site. Thus, we obtained data from 3 sites: Leiden (4 subjects), Utrecht (2 subjects) and Copenhagen (2 subjects) for a total of 8 subjects. Overall the data quality from all three sites was excellent – line width of less than 10 Hz for all subjects and excellent SNR. All data were analyzed in one site (Leiden) using LCModel, the industry standard. Quantification was done vs. water reference without correction for CSF and proton density in different tissue types. The graph below shows the mean and standard deviations of the reliably quantifiable metabolites.

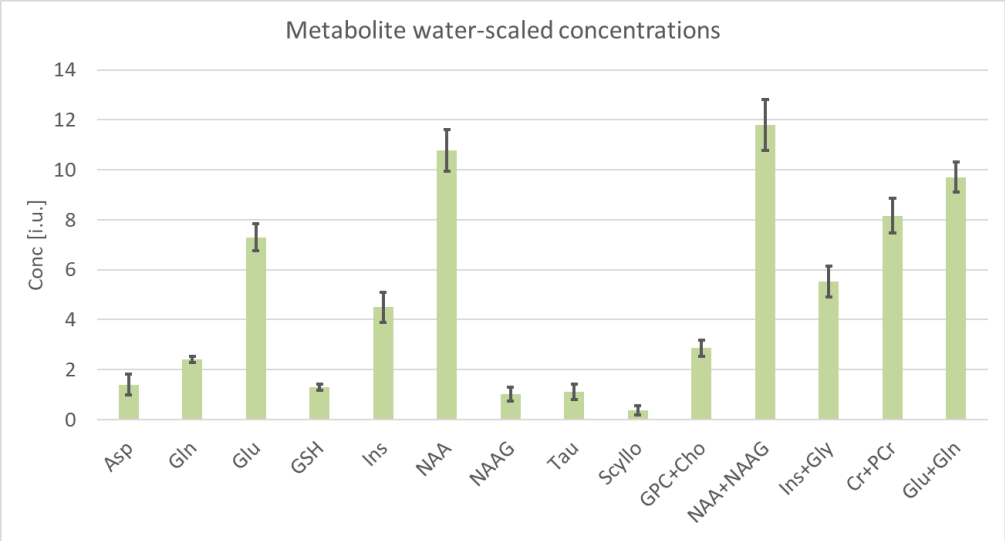

Across site variance was rather small. Also differences in the Cramer Rao Lower Bounds (CRLB) per metabolite across sites were small, attesting for very similar quality of spectra across the three sites.

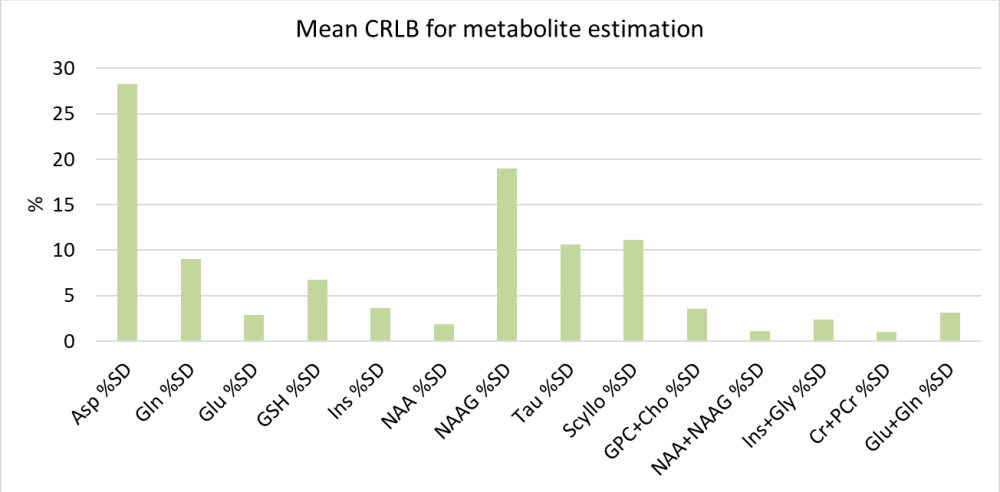

In particular it should be mentioned that the separate quantification of glutamine (Gln) and glutamate (Glu) was robust and consistent across subjects and sites. Same with the separate quantification of NAA and NAAG, even though the VOI consisted mostly of gray matter, where the NAAG concentrations are low. Below are the individual metabolite estimations for all subjects in all three sites, represented both as “absolute” concentration as well as their ratio to total creatine (Cr + PCr). While the ratio to Cr+PCR is consistent across sites, the absolute quantification, performed against the water signal from the same VOI, appear to contain some

bias. In particular, some of the metabolites were assigned higher concentrations in the LUMC site. This calls for careful examination of the acquisition of the water reference data in all sites and for careful harmonization, also with respect to other vendors.

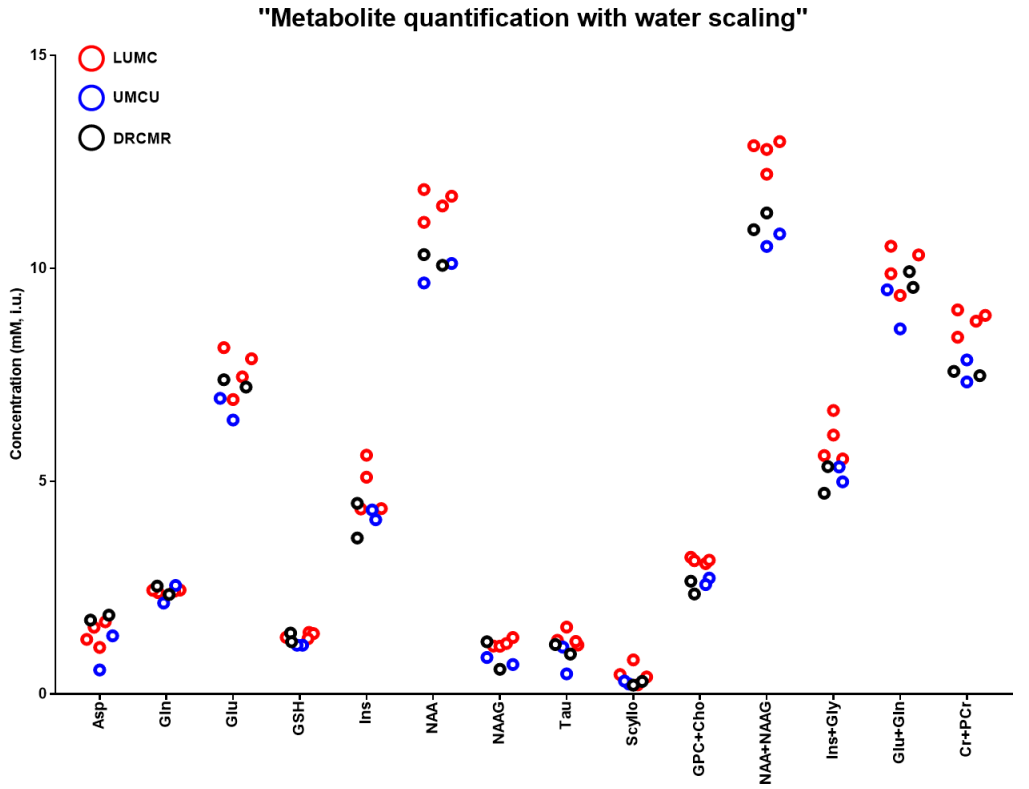

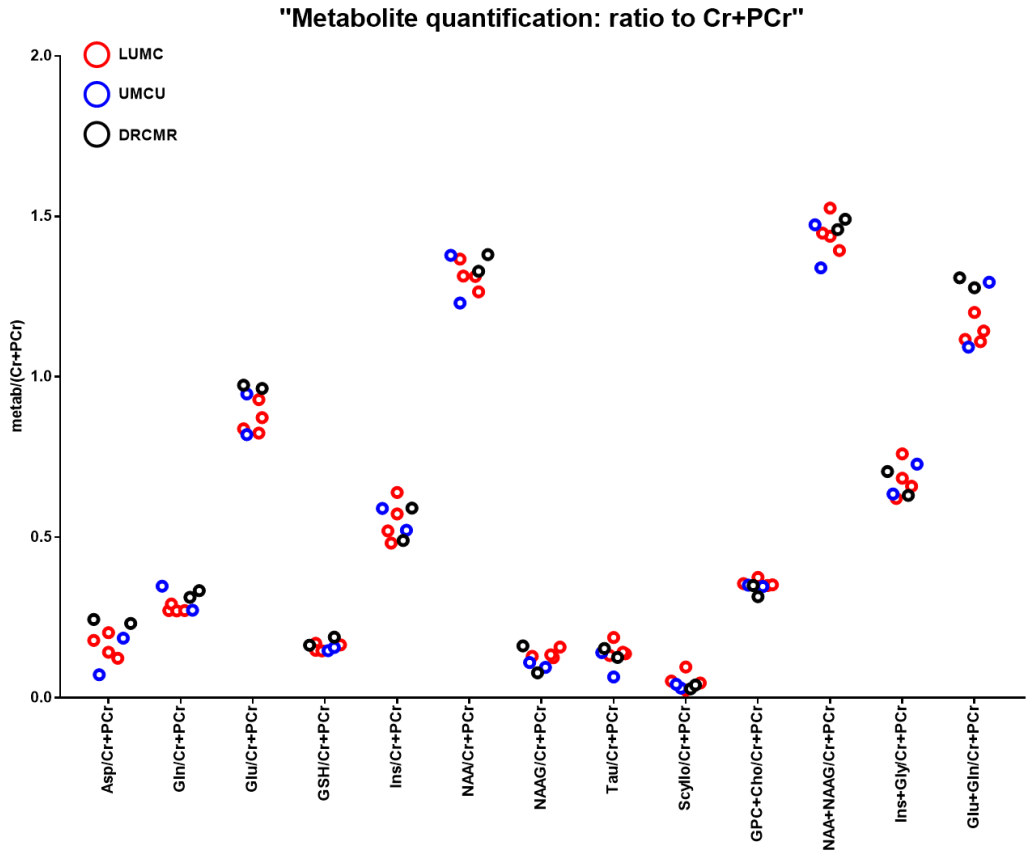

References

1. Zhang N, Song X, Bartha R, Beyea S, Arcy RD. *Advances in High-Field Magnetic Resonance Spectroscopy in Alzheimer ' s Disease*. Curr Alzheimer Res 2014;11:367–388.
2. Zaiss M, Bachert P. *Chemical exchange saturation transfer (CEST) and MR Z-spectroscopy in vivo: a review of theoretical approaches and methods*. Phys Med Biol 2013;58:221–269. doi: 10.1088/0031-9155/58/22/R221.
3. Wang H, Tan L, Wang HF, Liu Y, Yin RH, Wang WY, Chang XL, Jiang T, Yu JT. *Magnetic Resonance Spectroscopy in Alzheimer's Disease: Systematic Review and Meta-Analysis*. J Alzheimers Dis 2015;46:1049–1070. doi: 10.3233/JAD-143225.
4. Graff-Radford J, Kantarci K. *Magnetic resonance spectroscopy in Alzheimer's disease.* Neuropsychiatr Dis Treat 2013;9:687–696. doi: 10.2147/NDT.S35440.
5. Wang T, Xiao S, Li X, Ding B, Ling H, Chen K, Fang Y. *Using proton magnetic resonance spectroscopy to identify mild cognitive impairmen*t. Int Psychogeriatrics 2012;24:19–27. doi: 10.1017/S1041610211000962.
6. Bing Zhang, Tanis J. Ferman, Bradley F. Boeve, MD, Glenn E. Smith, Mandie Maroney-Smith, Anthony J Spychalla, David S. Knopman, Clifford R. Jack, Jr., Ronald C. Petersen and KK. *MRS in Mild Cognitive Impairment: Early Differentiation of Dementia with Lewy Bodies and Alzheimer's Disease*. J Neuroimaging 2015;25:269–274.
7. Bittner DM, Heinze H-J, Kaufmann J. *Association of 1H-MR spectroscopy and cerebrospinal fluid biomarkers in Alzheimer's disease: diverging behavior at three different brain regions.* J Alzheimers Dis 2013;36:155–63. doi: 10.3233/JAD-120778.
8. Kantarci K, Smith GE, Ivnik RJ, Petersen RC, Boeve BF, Knopman DS, Tangalos EG, Jack CR. *1H magnetic resonance spectroscopy, cognitive function, and apolipoprotein E genotype in normal aging, mild cognitive impairment and Alzheimer's disease*. J Int Neuropsychol Soc 2002;8:934–942.
9. Kantarci K, Lowe V, Przybelski SA, et al. *Magnetic resonance spectroscopy, ??-amyloid load, and cognition in a population-based sample of cognitively normal older adults*. Neurology 2011;77:951–958. doi: 10.1212/WNL.0b013e31822dc7e1.
10. Riese F, Gietl A, Zölch N, et al. *Posterior cingulate GABA and glutamate+glutamine are reduced in amnestic mild cognitive impairment and are unrelated to amyloid deposition and APOE genotype.* Neurobiol Aging 2015;36:53–59. doi: 10.1016/j.neurobiolaging.2014.07.030.
11. Mandal PK, Saharan S, Tripathi M, Murari G. Brain Glutathione Levels - *A Novel Biomarker for Mild Cognitive Impairment and Alzheimer's Disease*. Biol Psychiatry 2015;78:702–710. doi: 10.1016/j.biopsych.2015.04.005.
12. Modrego PJ, Fayed N, Artal J OS. *Correlation of findings in advanced MRI techniques with global severity scales in patients with Parkinson disease*. Acad Radiol 2011;18:235–241.
13. Emir UE, Tuite PJ, Öz G. *Elevated pontine and putamenal gaba levels in mild-moderate parkinson disease detected by 7 tesla proton* mrs. PLoS One 2012;7. doi: 10.1371/journal.pone.0030918.
14. Holmay MJ, Terpstra M, Coles LD, Tuite J. *N-acetylcysteine Boostss Brain and Blood Glutathione in Gaucher and Parkinson's Diseases*. Clin Neuropharmacol 2013;36:103–106. doi: 10.1097/WNF.0b013e31829ae713.
15. Tkáč I, Oz G, Adriany G, Uğurbil K, Gruetter R. *In vivo 1H NMR spectroscopy of the human brain at high magnetic fields: metabolite quantification at 4T vs. 7T*. Magn Reson Med 2009;62:868–879. doi: 10.1002/mrm.22086.
16. van de Bank BL, Emir UE, Boer VO, van Asten JJA, Maas MC, Wijnen JP, Kan HE, Oez G,

Klomp DWJ, Scheenen TWJ. *Multi-center reproducibility of neurochemical profiles in the human brain at 7 Tesla.* NMR Biomed 2015;28:306–316.
17. Koch KM, Rothman DL, de Graaf RA. *Optimization of static magnetic field homogeneity in the human and animal brain in vivo.* Prog Nucl Magn Reson Spectrosc 2009;54:69–96.
18. Fillmer A, Kirchner T, Cameron D, Henning A. *Constrained Image-Based B0 Shimming Accounting for "Local Minimum Traps" in the Optimization and Field Inhomogeneities Outside the Region of Interest*. Magn Reson Med 2015;73:1370–1380
19. Fillmer A, Vannesjo SJ, Pavan M, Scheidegger M, Pruessmann KP, Henning A. *Fast iterative pre-emphasis calibration method enabling third-order dynamic shim updated fMR*I. Magn Reson Med 2016;75:1119–1131
20. Nassirpour S, Chang P, Fillmer A, Henning A. *A comparison of optimization algorithms for localized in vivo B0 shimming.* Magn Reson Med 2017; Epub ahead of print (DOI: 10.1002/mrm.26758)
21. Adalsteinson E, Sullivan EV, Kleinhans N, Spielman DM, Pfefferbaum A. *Longitudinal decline oft he neuronal marker N-acetyl aspartate in Alzheimer's disease*. Lancet 2000;355:1696–1697
22. Kirchner T, Fillmer A, Tsao J, Pruessmann KP, Henning A. *Reduction of voxel bleeding in highly accelerated parallel 1H MRSI by direct control of the spatial response function*. Magn Reson Med 2015;73:469–480
23. Kirchner T, Fillmer A, Henning A. *Mechanisms of SNR and line shape improvement by B0 correction in overdiscrete MRSI reconstruction*. Magn Reson Med 2017;77:44–56
24. Nicolay K, Braun KPJ, de Graaf RA, Dijkhuizen RM, Kruiskamp MJ. *Diffusion NMR spectroscopy.* NMR Biomed 2001; 14:94–111.
25. Wood ET, Ronen I, Techawiboonwong A, Jones CK, Barker PB, Calabresi P, Harrison D, Reich DS. *Investigating axonal damage in multiple sclerosis by diffusion tensor spectroscopy*. J Neurosci 2012;32(19):6665–6669.
26. Ercan E, Magro-Checa C, Valabregue R, Branzoli F, Wood ET, Steup-Beekman GM, Webb AG, Huizinga TW, van Buchem MA, Ronen I. *Glial and axonal changes in systemic lupus erythematosus measured with diffusion of intracellular metabolites*. Brain 2016;139(Pt 5):1447–1457.
27. Mandal PK, Akolkar H TM. *Mapping of hippocampal pH and neurochemicals from in vivo multi-voxel 31P study in healthy normal young male/female, mild cognitive impairment, and Alzheimer's disease.* J Alzheimers Dis 2012;31:75–86.
28. Hattingen E, Magerkurth J, Pilatus U, Mozer A, Seifried C, Steinmetz H, Zanella F, Hilker R. Phosphorus and proton magnetic resonance spectroscopy demonstrates mitochondrial dysfunction in early and advanced Parkinson's disease. Brain 2009;132:3285–3297. doi: 10.1093/brain/awp293.
29. Du F, Zhu XH, Qiao H, Zhang X, Chen W. *Efficient in vivo 31P magnetization transfer approach for noninvasively determining multiple kinetic parameters and metabolic fluxes of ATP metabolism in the human brain*. Magn Reson Med 2007;57(1):103–114.
30. Mochel F, N'Guyen TM, Deelchand D, Rinaldi D, Valabregue R, Wary C, Carlier PG, Durr A, Henry PG. *Abnormal response to cortical activation in early stages of Huntington disease*. Mov Disord 2012;27(7):907–910.
31. Adanyeguh IM, Rinaldi D, Henry PG, Caillet S, Valabregue R, Durr A, Mochel F. *Triheptanoin improves brain energy metabolism in patients with Huntington disease.* Neurology 2015;84(5):490–495.
32. van Zijl PCM, Yadav NN. *Chemical Exchange Saturation Transfer (CEST): what is in a name and what isn't?* Magn Reson Med 2011;65(4):927–948.

33. Khlebnikov V, Geades N, Klomp DWJ, Hoogduin H, Gowland P, Mougin O.*Comparison of pulsed three‐dimensional CEST acquisition schemes at 7 tesla: steady state versus pseudosteady state*. Magn Reson Med 2017;77(6):2280–2287.
34. Xu J, Zaiss M, Zu Z, Li H, Xie J, Gochberg DF, Bachert P, Gore JC. *On the origins of chemical exchange saturation transfer (CEST) contrast in tumors at 9.4T*. NMR Biomed 2014;27(4):406–416.
35. Walkder-Samuel S, Ramasawmy R, Torrealdea F, Rega M, Rajkumar V, Johnson SP, Richardson S, Goncalves M, Parkes HG, Arstad E, Thomas DL, Pedley RB, Lythgoe MF, Golay X. *In vivo imaging of glucose uptake and metabolism in tumors*. Nature Medicine 2013;19:1067–1072.
36. Tietze A, Blicher J, Mikkelsen IK, Østergaard L, Trother MK, Smith SA, Donahue MJ. *Assessment of ischemic penumbra in patients with hyperacute stroke using amide proton transfer (APT) chemical exchange saturation transfer (CEST) MRI*. NMR Biomed 2014;27(2):163–174.
37. Schleich C, Bittersohl B, Miese F, Schmitt B, Müller-Lutz A, Sondern M, Antoch G, Krauspe R, Zilkens C. *Glycosaminoglycan chemical exchange saturation transfer at 3T MRI in asymtomatic knee joints.* Acta Radiol 2016;57(5):627–632.
38. Wells JA, O'Callaghan JM, Holmes HE, Powell NM, Johnson RA, Siow B, Torrealdea F, Ismail O, Walker-Samuel S, Golay X, Rega M, Richardson S, Modat M, Cardoso MJ, Ourselin S, Schwarz AJ, Ahmed Z, Murray TK, O'Neill MJ, Collins EC, Colgan N, Lythgoe MF. *In vivo imaging of tau pathology using multi-parametric quantitative MRI.* NeuroImage 2015;111: 369–378
39. Haris M, Cai K, Singh A, Hariharan H, Reddy R. *In vivo Mapping of Brain Myo-Inositol*. Neuroimage 2011; 54(3):2079–2085.

Subgroup contributors

Isabella Björkman-Burtscher; Fawzi Boumezbeur; Ariane Fillmer; Agnes Floel; Theresa Köbe, Penny Gowland; Bernd Ittermann; Mark Ladd; Armin Nagel; Florian Schubert; Hartwig Siebner; Michela Tosetti; Alexandre Vignaud; Andrew Webb

G. Quality assurance (QA), standard operating procedures (SOP), safety & multivendor harmonization

Subgroup coordinators: *Oliver Kraff, Stuart Clare*

Harmonization of protocols, SOPs and quality assessment is a large, but essential undertaking that is necessary before multi-centre trials can commence. There are three main hurdles to overcome in achieving this:

1. *Working across institutions:* Since the implementation of SOPs relies heavily on how these interface with the working practices of the individual institution, such SOPs need to be tight enough to enable consistency, but loose enough to allow local working practices to be followed without significant extra resource.
2. *Working across vendors:* Different vendors will have their own implementation of imaging pulse sequences and image reconstruction methods, so attempts to standardise protocols for imaging and quality assurance need to consider the limitations of each vendor, without necessarily accepting a 'lowest common denominator' solution.
3. *Working across regulatory bodies:* Whilst much is known about MR safety in general, scanning at 7T poses some safety concerns where the potential risks are not always known. Since safety is overseen by different regulatory bodies in different institutions, regions and countries, a common policy is not easy to achieve.

Work in addressing these hurdles has already begun within national networks.

German Ultrahigh Field Imaging (GUFI) Network

The GUFI network was founded at the end of 2013 with the aid of the German Research Foundation (DFG) for an initial period of three years which has been recently extended for another three years until 12/2019. All 11 German UHF sites are participating. In addition, Vienna (A) and Maastricht (NL) have joined the GUFI network at their own cost to contribute their experience and profit from the community.

The overall goal of GUFI is to facilitate and harmonize the work of the German UHF sites that all use MR systems from a single vendor (Siemens). A major topic within the network is quality assurance (QA) as it has emerged as a critical issue for UHF systems and a topic of common interest to all GUFI members, and in particular for planned multi-center studies. GUFI has implemented a common QA protocol to assess coil and system performance based on SNR, B1+, noise, and stability measures. High agreement was found between the sites, but the protocol also revealed hardware and calibration faults at some sites undetected before. A common QA phantom with realistic properties to compare inter-site data has been developed and will be distributed to all participating sites until end of 2017. A web based reporting system with normative performance data will be established until March 2018.

In addition, system reproducibility in human subjects has been compared within the network in a study targeting toward validating multicenter brain imaging at 7T, known as the "traveling heads" study [1]. High reproducibility was found at all sites, but differences in inter-site versus intra-site reproducibility were identified that could be correlated to hardware differences between the individual sites.

Within the first funding period, access procedures for both internal and external researchers have been harmonized between sites and a consensus guideline document has been formulated that

gives basic recommendations regarding access procedures and rules [2].

The GUFI partners have tried to clarify ethical, regulatory, liability, and safety issues common to all UHF MR sites. One important objective was a common guideline for dealing with subjects with passive implants. To date, very few medical implants have been certified as MR-safe or MR-conditional at 7T. However, as clinical applications become increasingly prominent, it becomes critical to define criteria under which individuals with implants can be included in research studies. The GUFI partners defined and signed a consensus recommendation for dealing with passive implants, including a flowchart with decision boxes to standardize decision making regarding whether a measurement at UHF MRI can be performed safely [3]. The network currently establishes a database with information on implant safety assessments, publications and history of safe use to share knowledge and experience on this topic among the GUFI partners. Safety aspects are in general of major concern when dealing with UHF MRI, and further harmonization is planned for the safety training of UHF MR users.

UK7T Network – Cambridge, Cardiff, Glasgow, Nottingham, Oxford

Established in 2015 and funded by the UK Medical Research Council, this network aims to develop a platform for multi-centre trials at 7T to be run. One of the key features is the desire to address the multi-vendor issue and produce work-horse protocols that are matched, as far as practicable, across the three variants of scanners available within the network (Phillips and two Siemens platforms).

Borrowing heavily from the work of the GUFI consortium the following protocols are currently under comparison in a 'travelling head' study.

- MPRAGE – 0.7 mm isotropic, ~6:30 min protocol
- MP2RAGE/PSIR – 0.7 mm isotropic, ~10 min protocol
- T2star-weighted - 0.7 mm isotropic, ~10 min protocol
- EPI – whole brain, multiband factor 4, TR < 1 sec
- B1 mapping - DREAM

Protocol harmonisation has included sharing of a custom RF inversion pulse across all sites, but otherwise uses vendor supplied reconstruction methods. Multiband sequences are provided by different third parties and comparisons are ongoing.

The outcome of the traveling heads comparison is expected by the early 2018, but an initial pilot shows that, as well as matching protocol parameters as much as possible, it is essential to standardise the various calibration steps (Tx power, B0 shim) that the scanner undertakes, in order to improve uniformity. A review of the data acquired so far indicates that standard structural scanning using an MP2RAGE/PSIR method can be made to be uniform across sites, but EPI based sequences are harder to standardise - particularly when slice acceleration (multiband) approaches are used.

Lessons from the pilot are being incorporated into the full travelling heads study and will be shared with the wider networks.

QA procedures are also being developed by the UK7T network. At present the composition of a common phantom for 7T MRI is being evaluated, with the expectation that QA procedures across all sites are in place by December 2017.

The UK7T network has started a dialogue between scientists and clinicians on how to increase our understanding of what is safe to scan at 7T. Studying the older population brings with it

additional challenges, highlighted by a recent UK7T analysis that showed that over 50% of research participants over 50 are likely to have a surgery that may have left metal in the body. Whilst many of these implants or clips may be safe to scan, the body of evidence is not large at the moment. The network is looking to identify surgeries and implants that can be scanned safely, and identify where further research would be beneficial.

EUFIND

A survey among the EUFIND sites showed that there are 12 sites operating on a Siemens system, 5 on a Philips system, and 2 sites are using a GE system. While all sites except one are equipped with the same RF head coil with 32 receiver channels (1 site uses a 24-channel version of the RF head coil), there are some differences on the transmit side between Siemens and Philips/GE sites. In addition, the survey revealed large differences with regard to the available gradient strength within the group of Siemens systems, allowing between 38 mT/m and 80 mT/m. Latter will have a large impact on the harmonization of protocols.
First results from the pilot-study showed an overall good image quality across sites and vendors but also revealed that the protocol harmonization needs further improvements, especially with regard to transmitter calibration and selecting similar RF pulses.
Combined with expected results from the UK7T travelling heads study, the EUFIND study will add value for harmonization efforts in general and 7T cross-vendor comparisons in detail.
In addition, the experiences from both national network's QA procedures will be shared and merged within the EUFIND network, as will be the experiences with implants across sites since this will be a major aspect for the particular study population.

References:

1. Voelker, M.N., et al., *The traveling heads: multicenter brain imaging at 7 Tesla.* MAGMA, 2016. **29**(3): p. 399-415.
2. German Ultrahigh Field Imaging (GUFI), *Recommendations regarding access procedures and user access rules at German ultra-high-field sites*, 2015, http://www.mr-gufi.de/images/documents/Access_method_and_user_access_rules_at_UHF.pdf
3. German Ultrahigh Field Imaging (GUFI), *Approval of subjects for measurements at ultra-high-field MRI*, 2015, http://www.mr-gufi.de/images/documents/Approval_of_subjects_for_measurements_at_UHF.pdf

Subgroup contributors

Isabella Björkman-Burtscher; Richard Bowtell; Marie Chupin; Emrah Duzel; Jeroen Hendrikse; Bernd Ittermann; Oliver Kraff; Mark Ladd; Armin Nagel; Thoralf Niendorf; Harald Quick; Esben Thade Petersen; Oliver Speck; Tony Stöcker; Michela Tosetti; Andrew Web

4. Concluding Remarks

Twenty-two 7 Tesla MR sites have joined the EUFIND working group. Within a period of 12 months, the EUFIND working group

- identified specific opportunities that a joint 7T network can provide in the areas of high-resolution anatomy, functional imaging, vascular lesion and vascular system assessment, quantitative susceptibility weighted imaging and spectroscopy
- agreed on sequences that are suitable to address these opportunities
- implemented a pilot-study to verify these sequences
- implemented an infrastructure and procedures for exchanging data across sites
- analysed the data from the pilot-study
- formulated a tractable short-term roadmap to advance the utility of 7T in neurodegeneration research and clinical application.

Development of the EUFIND network

After EUFIND began its work end of 2016, additional 7T sites joined. These include Marseille and Amsterdam. In addition, we are pleased to be able to include a US partner site in Wisconsin/Milwaukee. This opens the possibility to address the challenges of conducting 7T research projects across Europe and the US. These sites are representative of the global distribution of 7T scanners.

The EUFIND network according to vendors

Siemens	Philips	GE
Bonn	Copenhagen	Pisa
Essen	Nottingham	Wisconsin/Milwaukee
Würzburg	Lund	
Leipzig	Leiden	
Erlangen	Utrecht	
Heidelberg	Amsterdam	
Berlin		
Magdeburg		
Paris		
Marseille		
Cambridge		
Oxford		
Cardiff		
Glasgow		

Short-term opportunities in EUFIND

The EUFIND subgroups provide recommendations regarding high-resolution anatomy sequences, high-resolution fMRI, high-resolution assessment of vessel pulsatility, high-resolution QSM and spectroscopy. The sequences pushed the technical boundaries of what can be achieved with 7T in multi-centre studies. The protocol was developed in consensus. The result marks a major achievement of the working group, which contains a relevant portion of the global expertise in the field of 7T neuroimaging. The working group wanted to be ambitious in exploring the capabilities of the 7T technology in order to be able to identify areas where a major advance beyond available 3T technology is feasible. Consequently, the protocol implemented in EUFIND goes far beyond what can be achieved within 3T networks. The group identified and focused on methods with the highest potential at high field. At the same time, we have agreed not to focus on areas, where the benefit of 7T is less certain, such as diffusion tensor imaging.

Pilot-study

Subgroup recommendations for sequences were implemented in a pilot-study. Thirteen of the 7T sites were able to implement the pilot-study protocols and provide human subject data within the very short time frame of the JPND project. This is a remarkable success given that conducting a

pilot-study went far beyond the scope of the working group and no funding was provided to support this effort. Also, several sites have only recently received their scanner hardware or had a major focus on other organ systems. These sites have nevertheless made progress in adopting the joint protocol and it is quite foreseeable that the full network will soon be able to join the EUFIND roadmap implementation.

As can be seen in the reports from each topic subgroup, the pilot-study was a major success in revealing specific problems and challenges, which can now be effectively addressed in the near future. The pilot-study also helped to establish data exchange and communication channels across sites, and identified subgroup specific expertise in sequence implementation and data analysis. These developments will be major facilitators for achieving the next steps in our 7T roadmap.

As can be seen in the subgroup reports, each of these modalities were associated with specific challenges. For instance, the different modalities pose varying challenges for multivendor harmonization. While high-resolution anatomy sequences were relatively straightforward to implement across vendors, this appeared to be very challenging for imaging vessel pulsatility and spectroscopy. Having identified the specific problems will now enable EUFIND to efficiently explore them. In some cases this may require additional contributions and developments by the vendors.

The pilot study proved that it is possible to harmonize data acquisition across different institutions, system vendors and regulatory bodies. This effort built on and extended local projects (i.e. UK7T and GUFI) that previously demonstrated inter-site operability (Siemens only in GUFI) or multi-vendor comparison (two vendors in UK7T). For the first time all 7T vendors across multiple countries have been integrated into one study. The results clearly demonstrate the feasibility of multi-centre, multi-vendor 7T imaging. The harmonisation of sequences and protocols was largely possible, but further cross-platform efforts can improve data consistency. It was also identified that system adjustment procedures seem to contribute significantly to the differences. Overall, the data quality and homogeneity are very encouraging and the result surpasses our expectations at the start of EUFIND.

Roadmap of EUFIND

The EUFIND working group agreed that a roadmap for implementing 7T in a clinical research setting needs to accompany the ongoing and productive method development in the 7T field. We foresee a four-step process towards high impact multi-centre 7T research studies in neurodegeneration and even clinical application:

First, common sequences and SOPs need to be implemented as per the recommendations from all subgroups. As outlined above, this process has almost been completed in EUFIND, including a pilot study.

Second, a proof-of-concept study needs to be conducted with healthy older adults in the age-range spanning the preclinical phase of AD (>50 - 70 years).

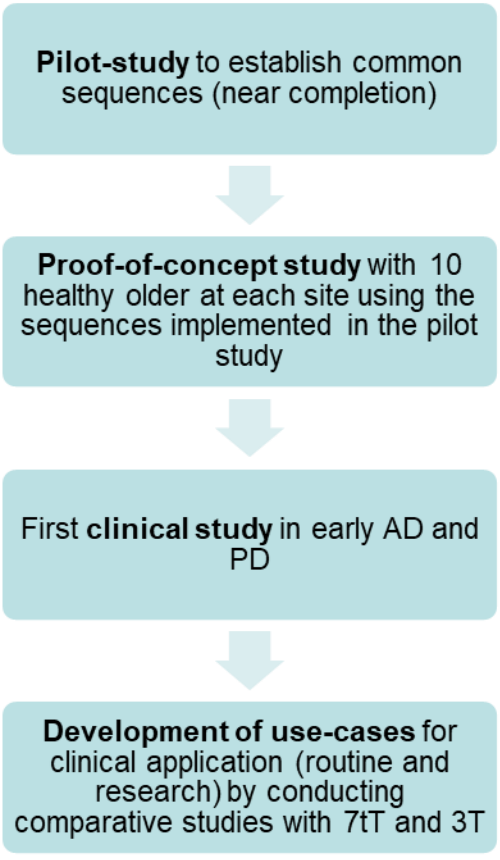

Third, a first clinical study with MCI, early AD or PD patients needs to be conducted to establish the planned readouts in a clinical population.
Fourth, on the basis of the developments achieved in phases 1 to 3, use-cases can be developed by conducting comparative studies in EUFIND using 3T and 7T.

Given the considerable progress that was achieved in EUFIND in establishing subgroups, joint protocols and pilot data, EUFIND members decided to continue beyond the funding period by organizing a third meeting in January 2018 in Berlin. During that meeting, the pilot-data will be discussed in detail and plans will be made for a proof-of-concept study as a preparation for a clinical study. The preliminary roadmap for this process is as follows:

Goal	Timeline	Status
Joint protocol	2017	Implemented
Pilot data (2 per site)	Until October 2017	Completed from 12 sites
Proof-of-concept study 10 adults per site (five 50-60 years + five 60-70 years)	Until mid 2018	In preparation. Final protocol definition during next EUFIND meeting Jan. 2018
First patient study (early AD)	End of 2018	Discussing design

Summary
The EUFIND network made considerable progress in the multi-site implementation of imaging sequences which push the boundaries of resolution that can currently be achieved. There are still challenges for multivendor harmonization that need to be overcome. Also, at the resolution that now can be achieved in EUFIND, movement correction remains a major challenge. EUFIND is in the best position to solve this challenge, at least for some sequence modalities, in the near future. We anticipate that the work conducted in EUFIND will be a major driver for advancing clinical neuroimaging research using 7T and for identifying use-cases for clinical routine applications in neurodegeneration.

5. Working Group Members

Coordinators:

Emrah Düzel
E: emrah.duezel@dzne.de
T: +49 391-67 25050

Oliver Speck
E: oliver.speck@ovgu.de
T: +49 391-6117-113

Contributors:

Annemette Løkkegaard, Hvidovre Hospital, University of Copenhagen, Danish Research Centre for Magnetic Resonance, Denmark

Esben Thade Petersen, Hvidovre Hospital, University of Copenhagen, Danish Research Centre for Magnetic Resonance, Denmark

Hartwig Siebner, Hvidovre Hospital, University of Copenhagen, Danish Research Centre for Magnetic Resonance, Denmark

Anne Bertrand, ICM, Paris, France

Hugues Chabriat, University Hospital Lariboisière, Paris, France

Marie Chupin, ICM, Paris, France

Olivier Colliot, University Salpêtrière Hospital, Paris, France

François De Guio, University Hospital Lariboisière, Paris, France

Bruno Dubois, University Salpêtrière Hospital, Paris, France

Stéphane Epelbaum, University Salpêtrière Hospital, Paris, France

Eric Jouvent, University Hospital Lariboisière, Paris, France

Alexandre Vignaud, Neurospin, Saclay/Paris, France

Mathieu Ceccaldi, Neurology and Neuropsychology Department, Aix-Marseille University, La Timone Hospital, Marseille, France

Ludovic de Rochefort, Centre for Magnetic Resonance in Biology and Medicine, Aix-Marseille University, CNRS, Marseille, France

Alexandre Eusebio, Neurology and Movement Disorders Department, Aix-Marseille University, La Timone Hospital, Marseille, France

Olivier Girard, Centre for Magnetic Resonance in Biology and Medicine, Aix-Marseille University, CNRS, Marseille, France

Maxime Guye, Centre for Magnetic Resonance in Biology and Medicine, Aix-Marseille University, CNRS, Marseille, France

Adil Maarouf, Centre for Magnetic Resonance in Biology and Medicine, Aix-Marseille University, CNRS, Marseille, France

Jean-Philippe Ranjeva, Centre for Magnetic Resonance in Biology and Medicine, Aix-Marseille University, CNRS, Marseille, France

Wafaa Zaaraoui, Centre for Magnetic Resonance in Biology and Medicine, Aix-Marseille University, CNRS, Marseille, France

David Berron, Institute for Cognitive Neurology and Dementia Research (IKND), University of Magdeburg, Germany

Cornelius Deuschl, University Hospital Essen, Germany

Martin Dichgans, Institut für Schlaganfall- und Demenzforschung, University of Munich, Germany

Emrah Düzel, German Center for Neurodegenerative Diseases, University of Magdeburg, Germany

Arturo Cardenas-Blanco, German Center for Neurodegenerative Diseases and Institute for Cognitive Neurology and Dementia Research (IKND), University of Magdeburg, Germany

Ariane Fillmer, Physikalisch-Technische Bundesanstalt (PTB), Berlin, Germany

Agnes Floel, Charite Neurology, Berlin, Germany

Bernd Ittermann, Physikalisch-Technische Bundesanstalt (PTB), Berlin, Germany

Frank Jessen, University of Cologne, Germany

Oliver Kraff, Erwin Hahn Institut, Radiologie Universitätsklinik, Essen, Germany

Mark Ladd, DKFZ, Heidelberg, Germany

Martin Lauer, Schwerpunkt Gerontopsychiatrie, Würzburg, Germany

Ulrike Lüken, Schwerpunkt Gerontopsychiatrie, Würzburg, Germany

Armin Nagel, Radiologie Universitätsklinik Erlangen, Germany

Peter Nestor, German Center for Neurodegenerative Diseases, University of Magdeburg, Germany

Thoralf Niendorf, Berlin Ultrahigh Field Facility, Max Delbrück Center for Molecular Medicine, Berlin, Germany

Oliver Peters, Charite Psychiatry, Berlin, Germany

Kerrin Pine, Max Planck Institute for Human Cognitive and Brain Sciences, Leipzig, Germany

Harald Quick, University Hospital Essen, Germany

Laura Schreiber, Deutsches Zentrum für Herzinsuffizienz, Würzburg, Germany

Matthias Schroeter, Max Planck Institute for Human Cognitive and Brain Sciences, Leipzig, Germany

Florian Schubert, Physikalisch-Technische Bundesanstalt (PTB), Berlin, Germany

Oliver Speck, University of Magdeburg, Germany

Tony Stöcker, German Center for Neurodegenerative Diseases, Bonn, Germany

Philipp Thomann, Klinik für Allgemeine Psychiatrie, Universitätsklinikum Heidelberg, Germany

Michael Uder, Radiologie Universitätsklinik Erlangen, Germany

Arno Villringer, Max Planck Institute for Human Cognitive and Brain Sciences, Leipzig, Germany

Christian Weimar, University Hospital Essen, Germany

Nikolaus Weiskopf, Max Planck Institute for Human Cognitive and Brain Sciences, Leipzig, Germany

Mirco Cosottini, University of Pisa, Italy

Mauro Costagli, Stella Maris Research Institute, Pisa, Italy Graziella Donatelli, University of Pisa, Italy

Michela Tosetti, Medical Physics and MR Biotechnology Lab, Pisa, Italy

Geert Jan Biessels, Brain Center Rudolf Magnus, University Medical Center Utrecht, the Netherlands

Mark van Buchem, Leiden University Medical Center, the Netherlands
Jeroen Hendrikse, Brain Center Rudolf Magnus, University Medical Center Utrecht, the Netherlands
Itamar Ronen, Leiden University Medical Center, the Netherlands
Yasin Temel, Maastricht University Medical Center, the Netherlands
Betty Tijms, Alzheimer Center VUMC, Amsterdam, the Netherlands
Kâmil Uludağ, University of Maastricht, the Netherlands
Andrew Webb, C.J. Gorter Center for High Field MRI, Leiden, the Netherlands
Jaco Zwanenburg, Brain Center Rudolf Magnus, University Medical Center Utrecht, the Netherlands
Serge Dumoulin, Spinoza Centre for Neuroimaging, Amsterdam, the Netherlands
Jeroen Siero, Spinoza Centre for Neuroimaging, Amsterdam, the Netherlands

Oskar Hansson, Lund University Bioimaging Center, Sweden
Lars Nyberg, Umea Center for Functional Imaging, Lund, Sweden
Greger Orädd, Umea Center for Functional Imaging, Lund, Sweden
Eric Westman, Lund University Bioimaging Center, Sweden
Bengt Winblad, Karolinska Institutet, Lund, Sweden

Julio Acosta-Cabronero, Wellcome Trust Centre for Neuroimaging, UCL, London, UK
Nin Bajaj, Nottingham University Hospital, UK
Richard Bowtell, Sir Peter Mansfield Imaging Centre, Nottingham, UK
Dennis Chan, University of Cambridge, UK
Stuart Clare, University of Oxford, UK
Gwenaëlle Douaud, University of Oxford, UK
Jozien Goense, University of Glasgow, Scotland School of Psychology, UK
Penny Gowland, Sir Peter Mansfield Imaging Centre, Nottingham, UK
Heidi Johanssen-Berg, FMRIB Centre, Oxford, UK
Clare Mackay, University of Oxford, UK
James Rowe, University of Cambridge, UK
Richard Wise, Cardiff University Brain Research Imaging Centre, UK

US American partner site:

Barbara Bendlin, Wisconsin Alzheimer's Disease Research Center, Madison

Sterling Johnson, Wisconsin Alzheimer's Disease Research Center, Madison

Tugan Muftuler, Associate Professor of Neurosurgery Medical College of Wisconsin Froedtert Hospital, Milwaukee